



2023 COASTAL MASTER PLAN

STORM SURGE AND WAVES MODEL IMPROVEMENTS

ATTACHMENT E1

REPORT: VERSION 02

DATE: JANUARY 2021

PREPARED BY: ZACH COBELL AND HUGH ROBERTS



COASTAL PROTECTION AND
RESTORATION AUTHORITY
150 TERRACE AVENUE
BATON ROUGE, LA 70802
WWW.COASTAL.LA.GOV

COASTAL PROTECTION AND RESTORATION AUTHORITY

This document was developed in support of the 2023 Coastal Master Plan being prepared by the Coastal Protection and Restoration Authority (CPRA). CPRA was established by the Louisiana Legislature in response to Hurricanes Katrina and Rita through Act 8 of the First Extraordinary Session of 2005. Act 8 of the First Extraordinary Session of 2005 expanded the membership, duties, and responsibilities of CPRA and charged the new authority to develop and implement a comprehensive coastal protection plan, consisting of a master plan (revised every six years) and annual plans. CPRA's mandate is to develop, implement, and enforce a comprehensive coastal protection and restoration master plan.

CITATION

Cobell, Z. & Roberts, H., (2021). 2023 Coastal Master Plan: Storm Surge and Waves Model Improvements. Version 2. (p. 56). Baton Rouge, Louisiana: Coastal Protection and Restoration Authority.

ACKNOWLEDGEMENTS

This document was developed as part of a broader Model Improvement Plan in support of the 2023 Coastal Master Plan under the guidance of the Modeling Decision Team:

- Coastal Protection and Restoration Authority (CPRA) of Louisiana – Elizabeth Jarrell (formerly CPRA), Stuart Brown, Ashley Cobb, Catherine Fitzpatrick (formerly CPRA), Krista Jankowski (formerly CPRA, David Lindquist, Sam Martin, and Eric White
- University of New Orleans – Denise Reed

This document was prepared by the 2023 Coastal Master Plan Storm Surge and Waves Team:

- Zach Cobell – The Water Institute of the Gulf
- Hugh Roberts – The Water Institute of the Gulf
- Elizabeth Jarrell – formerly CPRA
- Sam Martin – CPRA
- Eric White – CPRA
- Angelina Freeman – CPRA

The team would like to thank Max Agnew (United States Army Corps of Engineers, New Orleans District), Drs. Chris Massey and Noberto Nadal (United States Army Corps of Engineers, Engineering Research and Development Center, Coastal and Hydraulics Laboratory), and Andrew Cox (Oceanweather, Inc.) for assisting with access to data used in this report.

EXECUTIVE SUMMARY

This attachment describes the process to update the 2023 Coastal Master Plan models to both improve model skill in preparation for the upcoming Coastal Master Plan analysis, and create Advanced Circulation (ADCIRC) and Simulating Waves Nearshore (SWAN) model configurations that can be used for multiple surge and wave modeling applications within Louisiana. As part of efforts to improve the modeling for the 2023 Coastal Master Plan, exercises were undertaken to (1) simulate a series of hurricanes and calibrate model parameters for use in Louisiana which are useful to multiple Advanced Circulation (ADCIRC) modeling efforts statewide, (2) compute a reasonable initial condition for offshore water levels, and (3) conduct review of the riverine flow rates for use within the Coastal Master Plan so that they represent a statistically relevant value. To evaluate and calibrate model parameters, the ADCIRC and Simulating Waves Nearshore (SWAN) models were used to simulate seven historical hurricanes to analyze the performance of various parameterizations of air-sea drag and bottom friction. A review was conducted of how each parameterization was applied in prior storm surge modeling studies, including both those conducted throughout the country by Federal Emergency Management Agency (FEMA) contractors and those conducted locally, to determine which configurations showed the best performance in southern Louisiana. The seven historical hurricanes were compared using high-water marks and time series water levels to understand how varying the model parameters impacted both peak and transient parameters. An updated set of parameters is recommended for use in the 2023 Coastal Master Plan. These parameters are applicable not only for events which contain a well-defined hurricane vortex, but other events such as strong cold fronts or prolonged wind events. Additionally, the flow rates used in the Mississippi and Atchafalaya Rivers for synthetic hurricane events are updated. These updated flow rates are based on work conducted by the United States Army Corps of Engineers (USACE) to select a value that provides statistical return water levels approximate to a study which accounts for multiple flow rates being used for each hurricane in the suite. Lastly, the offshore water level initial condition is updated from the values used in the 2017 Coastal Master Plan. The 2017 Coastal Master Plan values were based on the post-Katrina Interagency Performance Evaluation Taskforce (IPET) analysis, while the updated value used for the 2023 Coastal Master Plan uses water levels recorded by the Coastwide Reference Monitoring System (CRMS) network.

TABLE OF CONTENTS

COASTAL PROTECTION AND RESTORATION AUTHORITY	2
CITATION	2
ACKNOWLEDGEMENTS	3
EXECUTIVE SUMMARY	4
TABLE OF CONTENTS	5
LIST OF TABLES	6
LIST OF FIGURES	6
LIST OF ABBREVIATIONS	9
1.0 INTRODUCTION	10
2.0 STORM SURGE AND WAVES MODEL PARAMETER DEVELOPMENT	11
2.1 Air-Sea Drag and Bottom Roughness Parameterization	11
Air-Sea Drag Formulations	12
Bottom Roughness Lower Limits	14
2.2 Parameterization Test Space	17
2.3 Hurricane Katrina Screening Results	18
2.4 Additional Storm Simulations	24
High-Water Marks Comparison	29
Timeseries Comparison	42
Recommendation	49
3.0 INITIAL AND BOUNDARY CONDITIONS	50
3.1 River Flow Rates	50
3.2 Offshore Water Levels	51
4.0 REFERENCES	55

LIST OF TABLES

Table 1. Initial list of parameter sets evaluated.	17
Table 2. Suite of historical storms used in performance evaluation.	18
Table 3. Hurricane Katrina screening analysis high-water mark comparisons. Note: parameter sets in bold were selected for additional analysis.	23
Table 4. Modeled high-water mark comparisons for Hurricane Katrina for the selected parameter sets.	29
Table 5. Modeled high-water mark comparisons for Hurricane Rita for the selected parameter sets.	31
Table 6. Modeled high-water mark comparisons for Hurricane Gustav for the selected parameter sets.	33
Table 7. Modeled high-water mark comparisons for Hurricane Ike for the selected parameter sets.	35
Table 8. Modeled high-water mark comparisons for Hurricane Isaac for the selected parameter sets.	37
Table 9. Aggregated high-water marks coastwide for all tested parameter sets.	42
Table 10. Aggregated high-water marks in Louisiana for all tested parameter sets.	42

LIST OF FIGURES

Figure 1. Interaction between air-sea stress and bottom stress.	11
Figure 2. Garratt-type (left) and Powell-type (right) air-sea drag parameterizations.	13
Figure 3. Patterns of wind (A), directional spread and air-sea drag (C, D) during Hurricane Katrina (Figure 10 in Holthuijsen 2012) showing the difference between the directional spreading based metric (C, E) and Wu (D, F) which very closely resembles Garratt.	14
Figure 4. Resulting bottom friction coefficient (C_d) for a Manning's n of 0.022 with different lower limits versus water depth.	16
Figure 5. Hurricane Katrina track denoting central pressure (mb).	19
Figure 6. Maximum water surface elevation from the simulation of Hurricane Katrina using parameter set 5 (ft; NAVD88 2009.55).	20
Figure 7. Maximum wave height and direction from the simulation of Hurricane Katrina using parameter set 5 (ft).	20
Figure 8. Hurricane Katrina comparison to observed high-water marks for parameter set 5.	21
Figure 9. Hurricane Katrina high-water mark regression for parameter set 5.	22

Figure 10. Storm tracks and associated central pressured used in the detailed analysis of the select subset of model parameterizations.	24
Figure 11. Maximum water surface elevation from the simulation of Hurricane Rita using parameter set 5 (ft, NAVD88 2009.55).	25
Figure 12. Maximum water surface elevation from the simulation of Hurricane Gustav using parameter set 5 (ft, NAVD88 2009.55).	26
Figure 13. Maximum water surface elevation from the simulation of Hurricane Ike using parameter set 5 (ft, NAVD88 2009.55).	26
Figure 14. Maximum water surface elevation from the simulation of Hurricane Isaac using parameter set 5 (ft, NAVD88 2009.55).	27
Figure 15. Maximum water surface elevation from the simulation of Hurricane Nate using parameter set 5 (ft, NAVD88 2009.55).	28
Figure 16. Maximum water surface elevation from the simulation of Hurricane Harvey using parameter set 5 (ft, NAVD88 2009.55).	28
Figure 17. Hurricane Rita comparison to observed high water marks for parameter set 5.	30
Figure 18. Hurricane Gustav comparison to observed high-water marks for parameter set 5.	32
Figure 19. Hurricane Ike comparison to observed high-water marks for parameter set 5.	34
Figure 20. Hurricane Isaac comparison to observed high-water marks for parameter set 5.	36
Figure 21. Aggregated coastwide high-water marks for parameter set 5.	38
Figure 22. Aggregated coastwide high-water mark regression for parameter set 5.	39
Figure 23. Louisiana-only aggregated high-water marks for parameter set 5.	40
Figure 24. Louisiana-only aggregated high-water mark regression for parameter set 5.	41
Figure 25. Modeled and observed water levels during Hurricane Katrina near the IHNC Lock. Parameter set numbers in the figure refer to Table 3.	44
Figure 26. Modeled and observed water levels during Hurricane Katrina near the IHNC Lock near the time of peak surge. Parameter set numbers in the figure refer to Table 3.	44
Figure 27. Hurricane Gustav modeled and observed water levels at Southwest Pass.	45
Figure 28. Hurricane Gustav modeled and observed water levels at Southwest Pass near the time of peak surge. Parameter set numbers in the figure refer to Table 3.	46
Figure 29. Hurricane Ike modeled and observed water levels at Sabine Pass. Parameter set numbers in the figure refer to Table 3.	46
Figure 30. Hurricane Ike modeled and observed water levels at Sabine Pass near the time of peak surge. Parameter set numbers in the figure refer to Table 3.	47
Figure 31. Hurricane Nate modeled and observed water levels at Pilottown. Parameter set numbers in the figure refer to Table 3.	47

Figure 32. Hurricane Nate modeled and observed water levels at Pilottown near the time of peak surge. Parameter set numbers in the figure refer to Table 3.	48
Figure 33. Hurricane Harvey modeled and observed water levels at Calcasieu Pass. Parameter set numbers in the figure refer to Table 3.	48
Figure 34. Hurricane Harvey modeled and observed water levels at Calcasieu Pass near the time of landfall. Parameter set numbers in the figure refer to Table 3.	49
Figure 35. Relative sea level trend at NOAA 8729840 in Pensacola, FL.	52
Figure 36. Computed mean sea level offset from NAVD88 2009.55 values at all available stations in the CRMS network.	53
Figure 37. Computed mean sea level offset from NAVD88 2009.55 at coastal stations in the CRMS network.	54

LIST OF ABBREVIATIONS

ADCIRC	ADVANCED CIRCULATION MODEL
AEP	ANNUAL EXCEEDANCE PROBABILITY
CFS.....	CUBIC FEET PER SECOND
CPRA	COASTAL PROTECTION AND RESTORATION AUTHORITY
CRMS	COASTWIDE REFERENCE MONITORING SYSTEM
FEMA	FEDERAL EMERGENCY MANAGEMENT AGENCY
GIWW	GULF INTRACOASTAL WATERWAY
HSDRRS.....	HURRICANE AND STORM DAMAGE RISK REDUCTION SYSTEM
IHNC	INNER HARBOR NAVIGATION CANAL
IPET	INTERAGENCY PERFORMANCE EVALUATION TASKFORCE
JPM-OS.....	JOINT PROBABILITY METHOD WITH OPTIMUM SAMPLING
NAVD88	NORTH AMERICAN VERTICAL DATUM OF 1988
NOAA	NATIONAL OCEANIC AND ATMOSPHERIC ADMINISTRATION
SWAN	SIMULATING WAVES NEARSHORE MODEL
USACE	U.S. ARMY CORPS OF ENGINEERS
USACE-MVN	U.S. ARMY CORPS OF ENGINEERS' NEW ORLEANS DISTRICT
USGS.....	U.S. GEOLOGICAL SURVEY

1.0 INTRODUCTION

Over the past 20 years research related to the modeling of hurricane-driven storm surge and waves, and subsequent advancements in the understanding of the physical processes that occur during these storm events, has led to the improvement of hydrodynamic and wave numerical models such as the ADvanced CIRCulation model (ADCIRC; Luetlich & Westerink, 2004). The master plan uses ADCIRC and the Simulating WAVes Nearshore (SWAN) model to simulate the impact of hurricanes on present and future landscapes with and without the presence of coastal restoration and protection projects. In advance of the 2023 Coastal Master Plan, the ADCIRC storm surge model and SWAN spectral wave model have been updated to account for advancements in research and model development that have occurred since model development was completed for the 2017 Coastal Master Plan. As part of these model updates, the master plan team coordinated with surge and wave model developers to conduct model tests for applications in coastal Louisiana. This ensures that parties conducting storm surge modeling within the state of Louisiana have a common set of assumptions about the underlying physics to begin from and allows for consistency across studies. Participants include those from the following organizations:

- CPRA team members supporting the 2023 Coastal Master Plan, Lowermost Mississippi River Management Plan, and other studies
- United States Army Corps of Engineers (USACE) Engineering Research and Development Center Coastal Hydraulics Laboratory
- Louisiana State University
- USACE New Orleans District (MVN)

This attachment describes the process to update the 2023 Coastal Master Plan models to both improve model skill in preparation for the upcoming master plan analysis, and create ADCIRC and SWAN model configurations that can be used for multiple surge and wave modeling applications within Louisiana. The model parameter testing process centered around extensive simulation of historical tropical storm events that made landfall in or near southern Louisiana.

Several parameters were considered for analysis as part of this work. These parameters were: air-sea drag parameterization, limits for bottom roughness, river flow rate, and offshore initial water levels. The air-sea drag and bottom roughness parameters represented changes to the numerical parameters in the model, balancing the stress terms enacted by wind and the ocean floor. The analysis of river flow rates and initial water levels was completed to establish assumptions that will be applied during the 2023 Coastal Master Plan to initialize the model under conditions representative of hurricane season.

2.0 STORM SURGE AND WAVES MODEL PARAMETER DEVELOPMENT

The values used to parameterize the interaction of the wind with the ocean surface (air-sea drag) and the resistance to flow caused by the seabed (bottom roughness) have been implemented in different ways over time within the ADCIRC model. The work to develop a consistent set of parameterization values for use in southern Louisiana, described in this document, includes the analysis of different combinations of parameters and concludes with recommended values based on those model setups that best replicate historical storm events.

2.1 AIR-SEA DRAG AND BOTTOM ROUGHNESS PARAMETERIZATION

The balance between air-sea drag and bottom roughness, and their associated stress vectors—air-sea stress and bottom stress—is a critical component of accurately predicting water levels generated by both tropical and non-tropical events, and has been a subject of particular interest in the ADCIRC community since Hurricane Ike (2008; Hope et al., 2013). Figure 1 shows a schematic for the interaction of the stress terms and lends insight into the importance of balancing the two parameters as part of model setup. Understanding this balance is critical, yet the measuring of these parameters during highly energetic events presents challenges and produces uncertainty in the parameterizations.

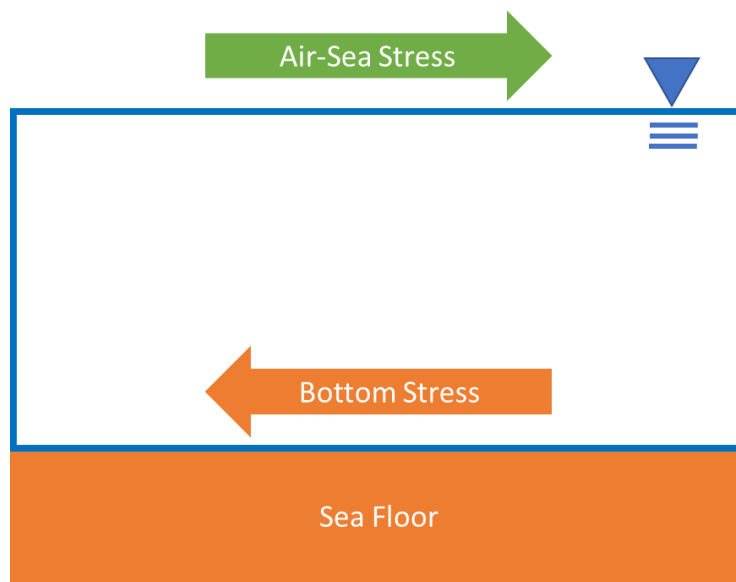


Figure 1. Interaction between air-sea stress and bottom stress.

AIR-SEA DRAG FORMULATIONS

Until 2012, the release version of the ADCIRC model code included the Garratt air-sea drag law (Garratt, 1977) with a user-defined upper limit. The SWAN wave model uses a near-identical formulation from Wu (1982). The Garratt air-sea drag law (1977) is shown in Equation (1) and Wu's formulation (1982) is shown in Equation (2).

$$C_d = \frac{1}{1000} \left(\frac{15}{20} + \frac{40}{600} U_{10} \right) \quad (1)$$

$$C_d = \frac{1}{1000} \left(\frac{16}{20} + \frac{39}{600} U_{10} \right) \quad (2)$$

where:

C_d	Air-sea drag coefficient
U_{10}	Wind speed at 10 meters above the surface

Historically, both Garratt and Wu's formulations have been applied in ADCIRC and SWAN respectively, using an upper limit to represent the wind speed at which the roughness of the sea surface begins to decrease due to high wind shear. However, neither of these equations directly account for the influence of waves on air-sea drag.

Analysis by Powell (2007) showed that air-sea drag coefficients vary dependent upon the location relative to the center of a hurricane and the forward direction of the storm, rather than having a uniform relationship computed throughout the storm's wind field. Powell's parameterization accounts for the differences in wave and wind direction by dividing the storm into three sectors. In the front right sector of the storm, where the counterclockwise winds of the hurricane and waves align, the drag coefficient is lower than in the front left sector of the storm where the wind and waves travel in opposite directions (Figure 2). This parameterized air-sea drag function was implemented into the ADCIRC model and used for validation studies including those conducted during the 2017 Coastal Master Plan (Dietrich et al., 2011b; Hope et al., 2013; Roberts & Cobell, 2017).

The Powell parameterization relies on the presence of a well-defined hurricane vortex within the model domain in order to make assumptions about the direction of wave travel. Later work by Holthuijsen (Holthuijsen et al., 2012; Figure 3) developed a parameterization that directly accounted for the direction of wave travel by using directional spreading as a metric which can be calculated directly using the SWAN wave model. This approach adds specificity to the air-sea interaction within the ADCIRC and SWAN models but does require additional scrutiny as part of model testing as a

Holthuijsen-type approach has not yet been applied in large-scale storm surge studies.

There are multiple air-sea drag configurations that can be used to simulate hurricane storm surge. To assess the optimal ADCIRC and SWAN model setup, multiple variations of Garratt-, Powell-, and Holthuijsen-type air-sea drag formulations were tested for this analysis to determine which formulation performed best through a wide range of event types for southern Louisiana. Note that SWAN always uses Wu when ADCIRC uses either Garratt or Powell.

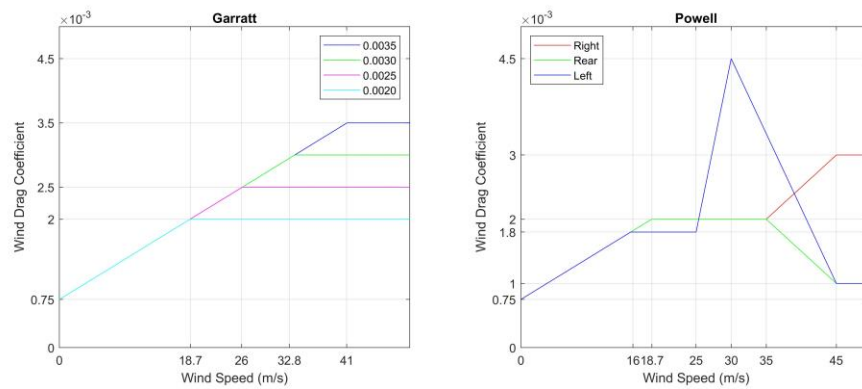


Figure 2. Garratt-type (left) and Powell-type (right) air-sea drag parameterizations.

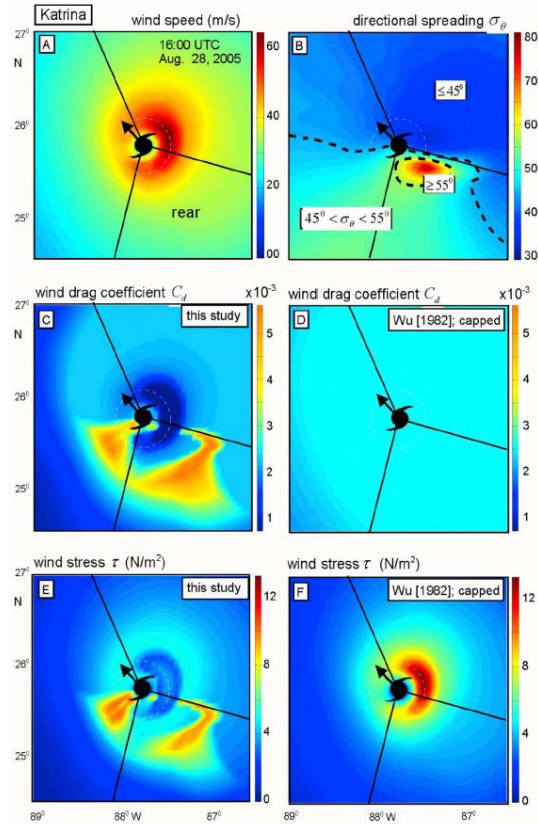


Figure 3. Patterns of wind (A), directional spreading and air-sea drag (C, D) during Hurricane Katrina (Figure 10 in Holthuijsen 2012) showing the difference between the directional spreading based metric (C, E) and Wu (D, F) which very closely resembles Garratt.

BOTTOM ROUGHNESS LOWER LIMITS

As with air-sea drag, the parametrization of bottom roughness can vary in ADCIRC. The ADCIRC model includes the option to use multiple types of bottom friction parameterizations (i.e., Manning's n , Chézy, and a spatially varying but temporally constant quadratic coefficient). Manning's n has been most widely applied for nearshore studies and was the parameterization used in this analysis. Manning's n is converted to a quadratic friction coefficient for use in the governing equations using Equation (3). The SWAN model uses a Madsen bottom friction formulation derived from the Manning's n coefficient specified in ADCIRC, which is converted to a friction length, K_N , in Equation (4).

$$C_d(t) = \frac{gn^2}{\sqrt[3]{h + \eta(t)}} \quad (3)$$

where:

$C_d(t)$	Quadratic friction coefficient as a function of time
g	Gravitational acceleration
n	Manning's n coefficient
$h + \eta(t)$	Total water depth as a function of time

$$K_N(t) = [h + \eta(t)]e^{-\left[1 + \frac{\kappa(h + \eta(t))^{1/6}}{n\sqrt{g}}\right]} \quad (4)$$

where:

$K_N(t)$	Roughness length as a function of time
$h + \eta(t)$	Total water depth as a function of time, assumed to be equivalent to hydraulic radius
κ	Von Karman constant (0.4)
n	Manning's n coefficient
g	Gravitational acceleration

Importantly, the quadratic friction coefficient applied in ADCIRC is dependent upon the cube root of the total water depth, which indicates that friction in the depth-integrated model is much higher in shallow areas and much lower in deep areas. Without a limit, this equation approaches zero for large depths in deep portions of the ocean, as shown in Figure 4.

Many applications of ADCIRC, including work conducted by the Federal Emergency Management Agency (FEMA) in Louisiana (Federal Emergency Management Agency Region Six, and the U.S. Army Corps of Engineers, 2008), set the lower limit of bottom roughness (C_d) to 0.0035. However, with this limit on bottom roughness, the ADCIRC model required a Garratt-based air-sea drag formulation with a drag coefficient higher than those documented in available literature to render model results that compared well to historical observations.

More recent studies included a bottom roughness lower limit less than 0.0035 in response to a 2011 USACE analysis of Hurricane Ike, which propagated along the Louisiana-Texas shelf (Hope et al., 2013; USACE, 2011). The Hurricane Ike analysis demonstrated that ADCIRC could not reliably replicate water level time series pre-landfall for model setups that included a high bottom roughness limit. Accordingly, the bottom roughness lower limits were reduced in ADCIRC and tested with varying air-sea drag formulations. Literature suggests likely explanations for low friction conditions during high wind events, including by Reid (1957). However, there is still active research underway in this area to directly include the interaction of wind speed and bottom roughness within the depth-integrated model. Building from USACE and Hope et al. studies in 2011 and 2013, the 2017 Coastal Master Plan study (Roberts & Cobell, 2017) used a lower limit of zero for C_d combined with a Powell-based air-sea

drag formulation. Similar to the USACE 2011 study, the 2017 Coastal Master Plan ADCIRC models demonstrated a high level of model skill and were able to capture pre-storm forerunner effects for Hurricane Ike.

Though the ADCIRC model validation conducted for the 2017 Coastal Master Plan study demonstrated a high level of skill using a Powell-based air-sea drag formulation and a bottom roughness lower limit of zero, the model parameters were re-examined in coordination with a broad group of ADCIRC users for southern Louisiana to determine a setup that is suitable for the 2023 Coastal Master Plan and other users. As described in the following section, lower limits of C_d , ranging from zero to 0.0035 (Figure 4) were tested in combination with multiple air-sea drag configurations to assess which formulation performed best through a wide range of event types for southern Louisiana.

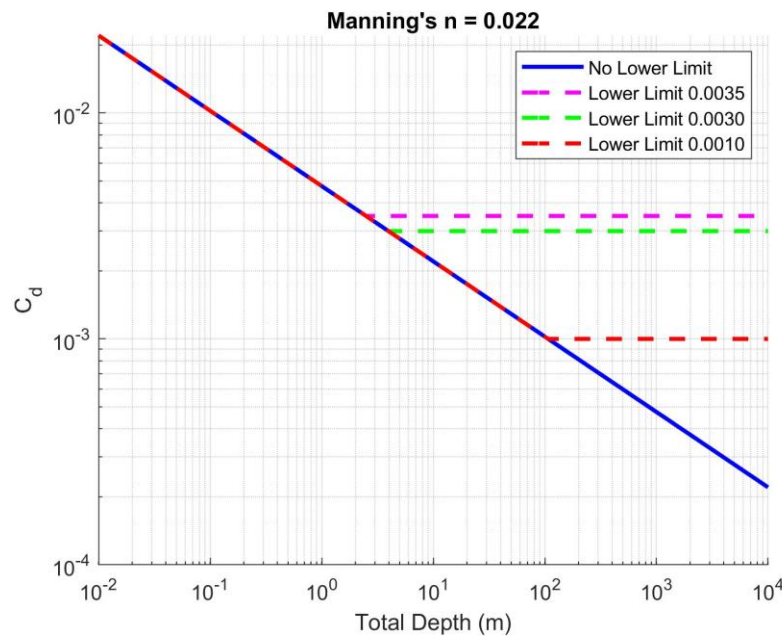


Figure 4. Resulting bottom friction coefficient (C_d) for a Manning's n of 0.022 with different lower limits versus water depth.

2.2 PARAMETERIZATION TEST SPACE

This section describes the tests completed to identify air-sea drag and bottom roughness parameterizations that are broadly applicable for use in Louisiana. The full parameter test space, shown in Table 1, was developed to examine a large number of air-sea drag and bottom roughness lower limit combinations.

The full parameter test space was initially examined with a simulation of Hurricane Katrina. The model results for Hurricane Katrina were compared to observational data to narrow the full parameter space to a subset of model parameterizations to be tested using a broader set of historical storms in Section 2.3. The set of historical storms used to test the subset of parameterizations, shown in Table 2, includes storms with varying sizes, intensities, and landfall locations.

Table 1. Initial list of parameter sets evaluated.

Parameter Set	Drag Formula	Air-Sea Drag Upper Limit	Bottom Roughness Lower Limit
1	Garratt	0.0020	0.000
2	Garratt	0.0020	0.001
3	Garratt	0.0020	0.003
4	Garratt	0.0025	0.000
5	Garratt	0.0025	0.001
6	Garratt	0.0025	0.003
7	Garratt	0.0030	0.000
8	Garratt	0.0030	0.001
9	Garratt	0.0030	0.003
10	Garratt	0.0035	0.000
11	Garratt	0.0035	0.001
*12	Garratt	0.0035	0.003
†13	Powell	n/a	0.000
14	Powell	n/a	0.001
15	Powell	n/a	0.003
16	Holthuijsen	n/a	0.000
17	Holthuijsen	n/a	0.001
18	Holthuijsen	n/a	0.003

*FEMA 2008

†2017 Coastal Master Plan

Table 2. Suite of historical storms used in performance evaluation.

Storm	Year
Katrina	2005
Rita	2005
Gustav	2008
Ike	2008
Isaac	2012
Nate	2017
Harvey	2017

2.3 HURRICANE KATRINA SCREENING RESULTS

Hurricane Katrina was used to screen the full parameter test space of air-sea drag and bottom roughness parameterizations listed in Table 1.

The simulation of Hurricane Katrina began on August 7, 2005 at 00:00 UTC. The simulation was initially forced with only astronomical tides and riverine inflows for 18-days to achieve a dynamic steady-state condition prior to the application of hurricane winds. Simulation of wind forcing began on August 25, 2005 00:00 UTC and continued until August 31, 2005 00:00. Following the end of the available wind data, a single additional day of simulation was used to allow the floodwaters to begin to recede. The storm track for Hurricane Katrina is shown in Figure 5.

High-water marks collected post-storm, which have been used in prior studies for model validation, were used for this analysis (Dietrich et al., 2011a; Federal Emergency Management Agency Region Six and the U.S. Army Corps of Engineers, 2008). Adjustments to the high-water marks to account for differences in datum, converting from NAVD88 2004.65 to NAVD88 2009.55, were made to align with the model datum using the National Oceanic and Atmospheric Administration's (NOAA) VDatum tool (Yang et al., 2010).

The maximum water surface elevation from the simulation of Hurricane Katrina, using parameter set 5 from Table 1 (Garratt drag formula, 0.0025 air-sea drag upper limit, 0.0010 bottom roughness lower limit), is shown in Figure 6, and the maximum wave height is shown in Figure 7. The comparison to observed high-water marks is shown in Figure 8 and Figure 9.

Table 3 includes a summary of the comparison to high-water marks for the full parameter test space listed in Table 1.

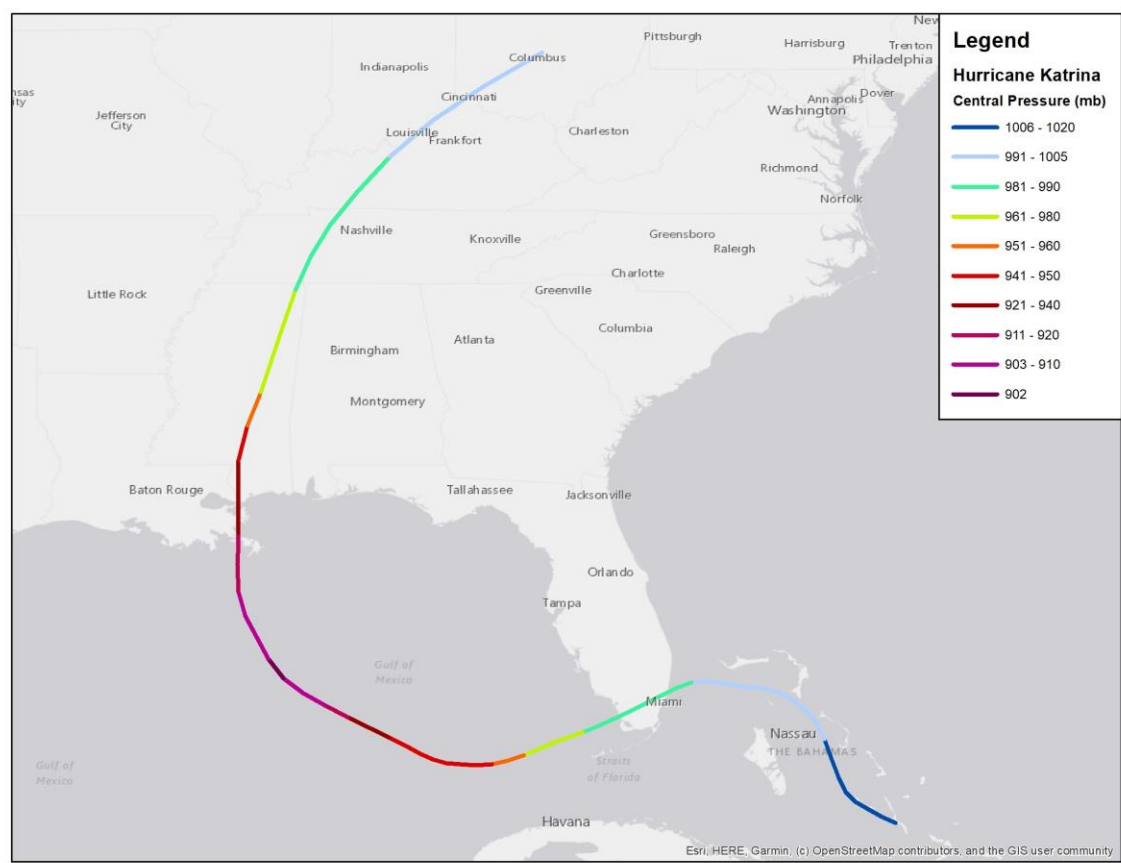


Figure 5. Hurricane Katrina track denoting central pressure (mb).

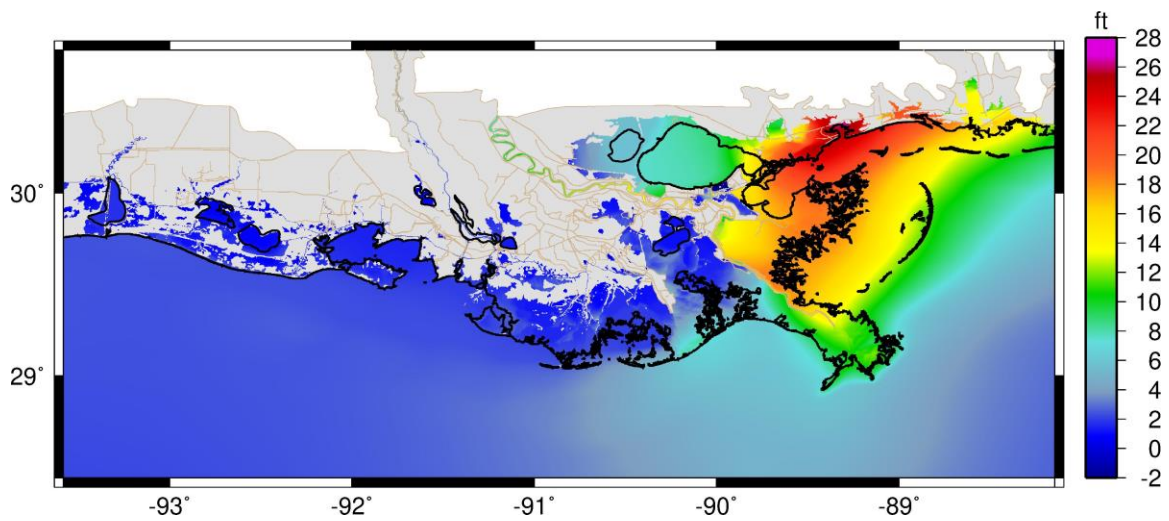


Figure 6. Maximum water surface elevation from the simulation of Hurricane Katrina using parameter set 5 (ft; NAVD88 2009.55).

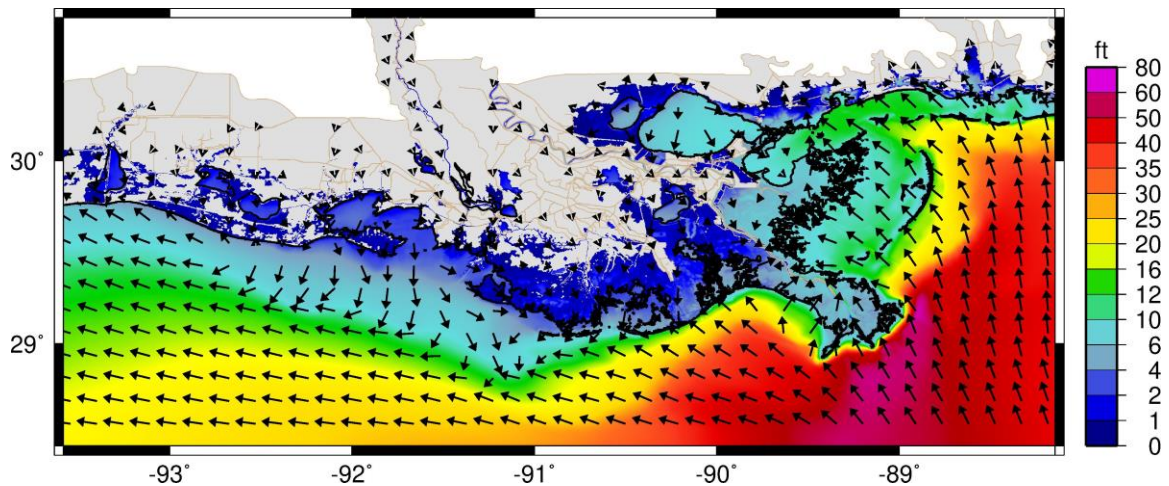


Figure 7. Maximum wave height and direction from the simulation of Hurricane Katrina using parameter set 5 (ft).

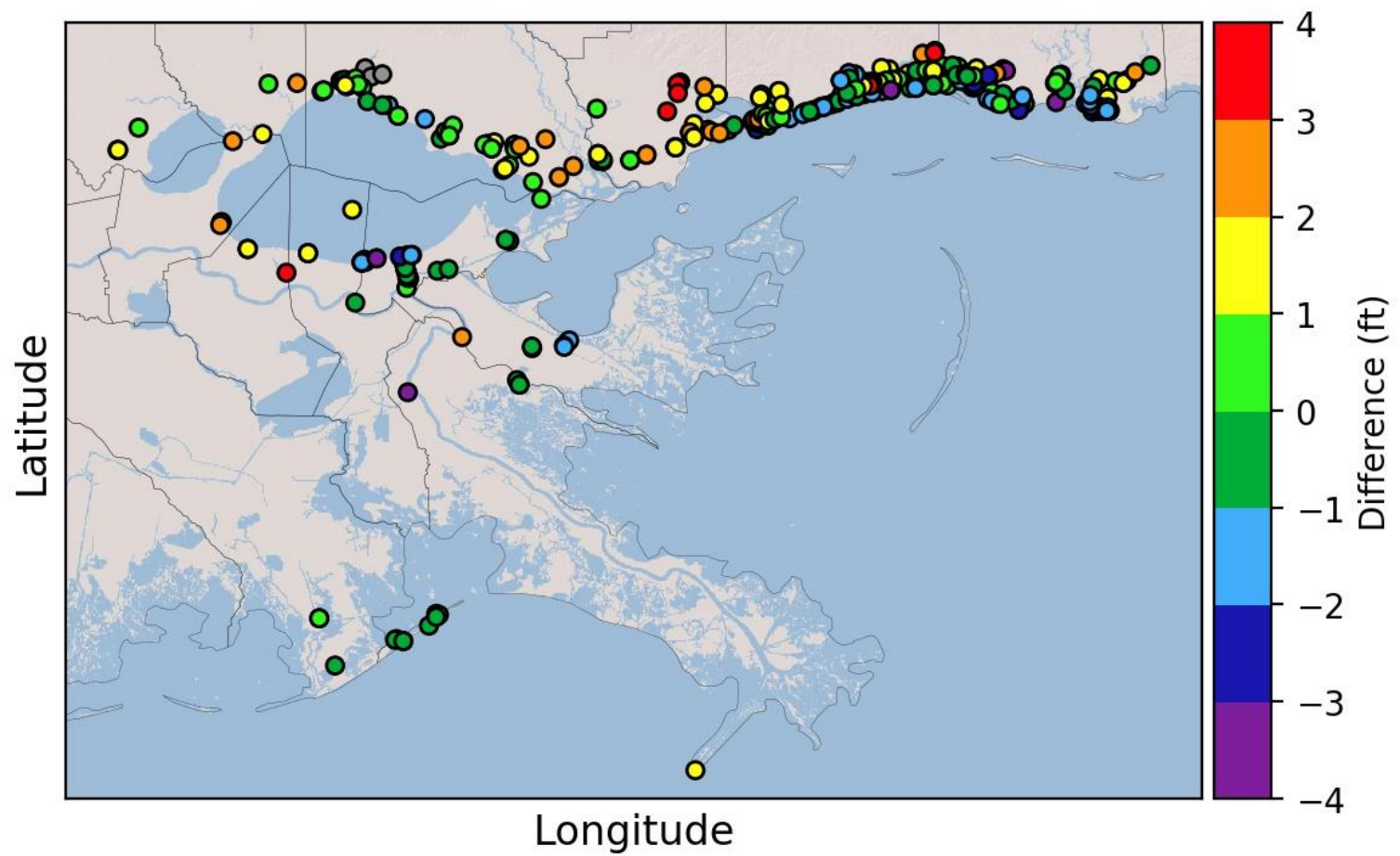


Figure 8. Hurricane Katrina comparison to observed high-water marks for parameter set 5.

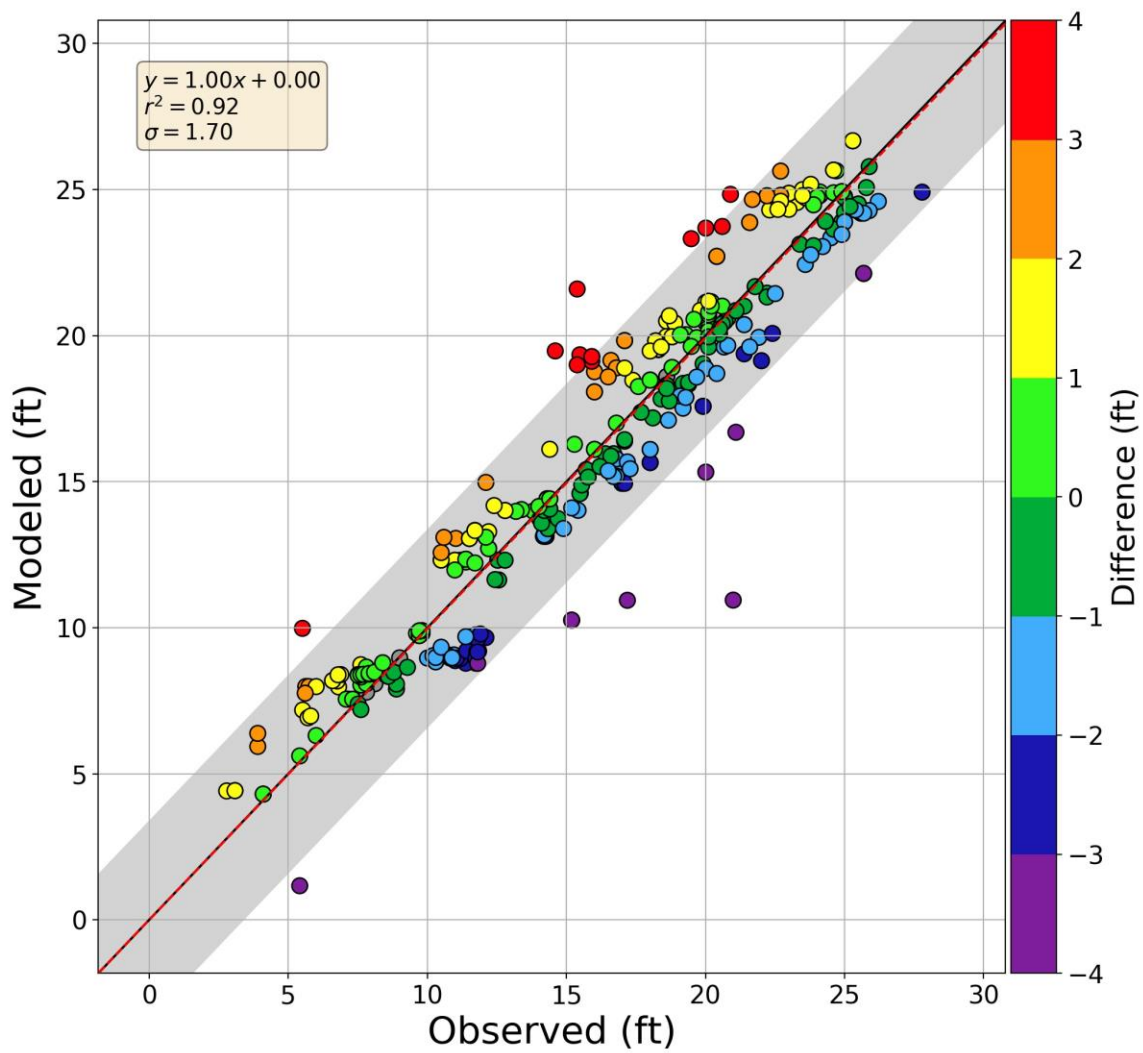


Figure 9. Hurricane Katrina high-water mark regression for parameter set 5.

Table 3. Hurricane Katrina screening analysis high-water mark comparisons.
Note: parameter sets in bold were selected for additional analysis.

Parameter Set	Drag Formula	Air-sea drag Limit	Bottom Friction Limit	Slope	R^2	σ
1	Garratt	0.0020	0.000	0.90	0.91	1.78
2	Garratt	0.0020	0.001	0.88	0.91	1.80
3	Garratt	0.0020	0.003	0.81	0.93	1.77
4	Garratt	0.0025	0.000	1.02	0.91	1.75
5	Garratt	0.0025	0.001	1.00	0.92	1.70
6	Garratt	0.0025	0.003	0.91	0.92	1.61
7	Garratt	0.0030	0.000	1.12	0.92	1.75
8	Garratt	0.0030	0.001	1.10	0.92	1.94
9	Garratt	0.0030	0.003	0.99	0.93	1.58
10	Garratt	0.0035	0.000	1.19	0.92	2.52
11	Garratt	0.0035	0.001	1.17	0.92	2.38
*12	Garratt	0.0035	0.003	1.05	0.93	1.80
†13	Powell	n/a	0.000	1.02	0.92	1.65
14	Powell	n/a	0.001	1.00	0.92	1.63
15	Powell	n/a	0.003	0.90	0.92	1.69
16	Holthuijsen	n/a	0.000	0.90	0.92	1.69
17	Holthuijsen	n/a	0.001	0.91	0.92	1.69
18	Holthuijsen	n/a	0.003	0.83	0.93	1.59

*FEMA 2008

†2017 Coastal Master Plan

Parameter sets 4, 5, 9, 12, 13, and 14 were selected for additional analysis based on the slope, correlation, and standard deviation values shown in Table 3. Selected parameter sets fall within a slope range of 0.95 to 1.05. Parameter set 12 was utilized during the 2008 FEMA study in Louisiana (Federal Emergency Management Agency Region Six, and the U.S. Army Corps of Engineers, 2008) and is representative of a legacy application of air-sea drag and bottom friction. Parameter set 13 was used in the 2017 Coastal Master Plan.

Note that the above screening analysis used ADCIRC version 53.05 and the subsequent analysis described use version 54.01. ADCIRC version 54.01 had not been released when the Hurricane Katrina screening analysis was conducted but contains an update to the calculation of the effect of directional roughness on wind which was deemed important to include for this analysis. Additionally, the 2023 Coastal Master Plan production simulations will use v54.01.

2.4 ADDITIONAL STORM SIMULATIONS

The set of seven historical hurricanes shown in Table 2 and Figure 10, including Hurricane Katrina, were used to further analyze the parameter sets 4, 5, 9, 12, 13, and 14 discussed above. Each of the seven historical storms were simulated using the six selected parameter sets to assess model performance compared to available observation data.

The historical hurricanes selected include storms with varying sizes, intensities, and landfall locations, including storms that both bypassed and that made landfall in Louisiana. While the bypassing storms may not have high-water mark data within southern Louisiana, gage networks from NOAA, United States Geological Survey (USGS), and CRMS were available for comparing to model time series and peak water surface elevation values for all storms.

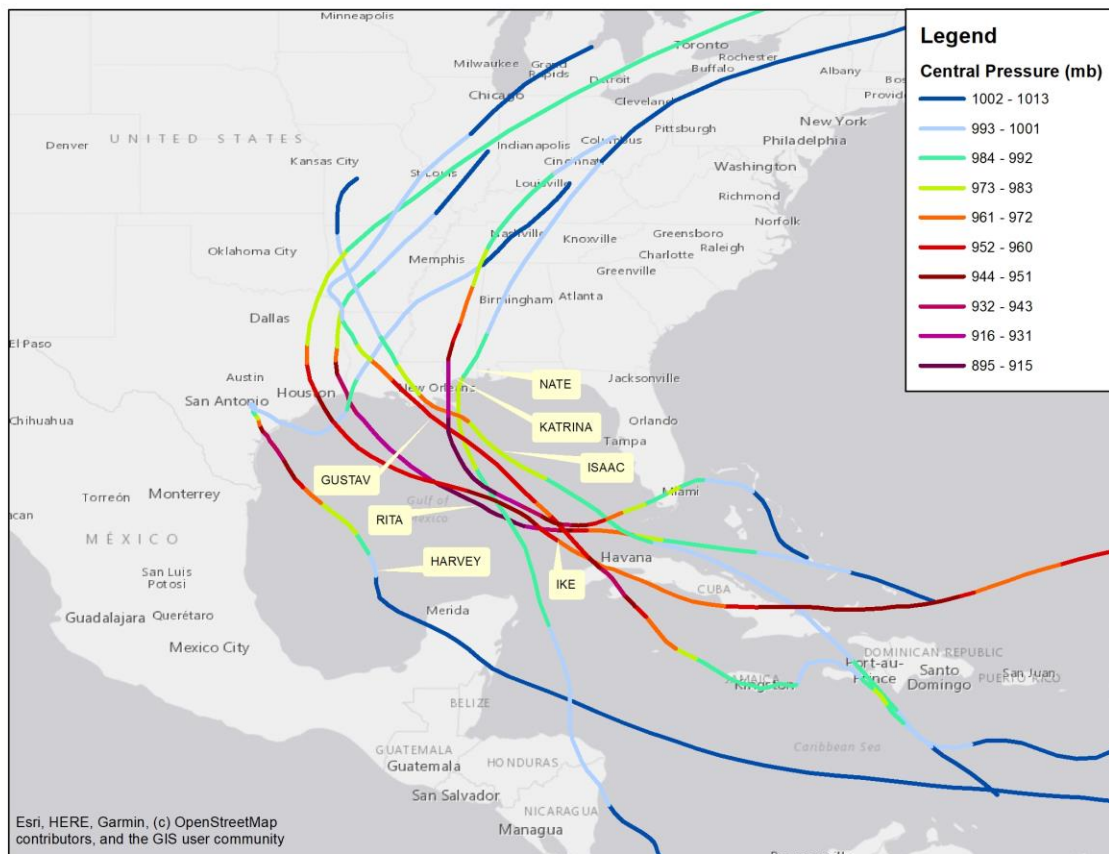


Figure 10. Storm tracks and associated central pressures used in the detailed analysis of the select subset of model parameterizations.

Hurricanes Katrina and Rita represent strong storms making landfall on the eastern and western portions of the state, respectively. Hurricane Gustav made landfall near the central part of the coast with moderate strength and Isaac made landfall near Barataria Bay with a slow, stalling, forward speed and moderate strength. Hurricane Ike was a strong storm that bypassed Louisiana and made landfall in Texas, but generated strong shore-parallel currents along the Louisiana-Texas shelf and is particularly informative as part of timeseries comparisons for parameter testing. Hurricane Harvey also made landfall in Texas, further southwest of Hurricane Ike's landfall location, though Harvey had a second landfall as a tropical storm in southwest Louisiana. Lastly, Hurricane Nate bypassed the Mississippi River delta before making landfall in the state of Mississippi.

Historical storm simulations were set up to be representative of the conditions when the storm occurred. River flow rates were modified using the USGS discharge gage at Baton Rouge for the Mississippi River and USGS gage at Simmesport for the Atchafalaya River. Offshore levels were set based upon the mean seasonal cycle recorded at Grand Isle by NOAA. Lastly, for simulations that occurred before the construction of the Hurricane and Storm Damage Risk Reduction System (HSDRRS) was completed, the mesh was modified to remove structures and projects that are part of this system: the Seabrook gate; Inner Harbor Navigation Canal (IHNC) Barrier; West Closure Complex; partial Morganza to the Gulf construction; and the Mississippi River Gulf Output Navigation Channel Closure.

Figure 11 through Figure 16 show the peak water surface elevations for each storm for simulations using parameter set 5. Note that Hurricane Katrina is shown in Figure 5 using ADCIRC v53.05.

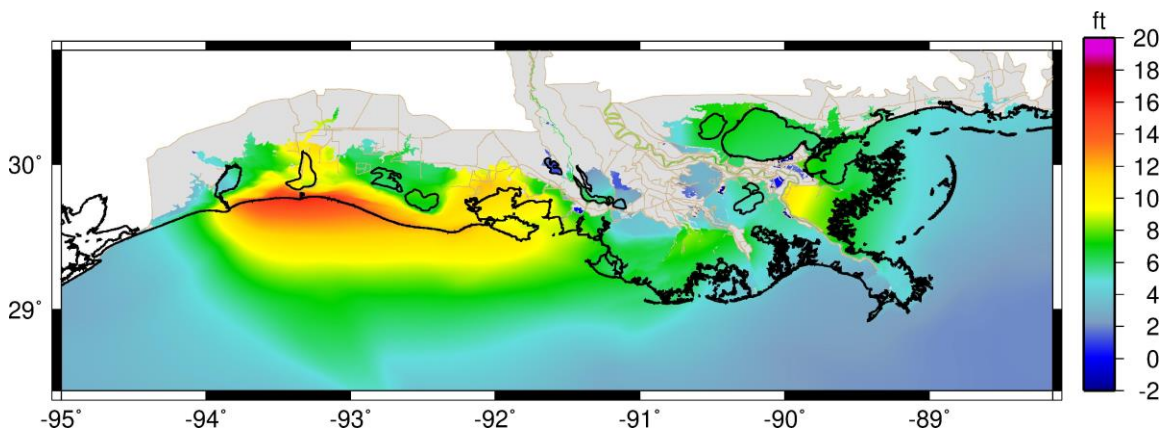


Figure 11. Maximum water surface elevation from the simulation of Hurricane Rita using parameter set 5 (ft, NAVD88 2009.55).

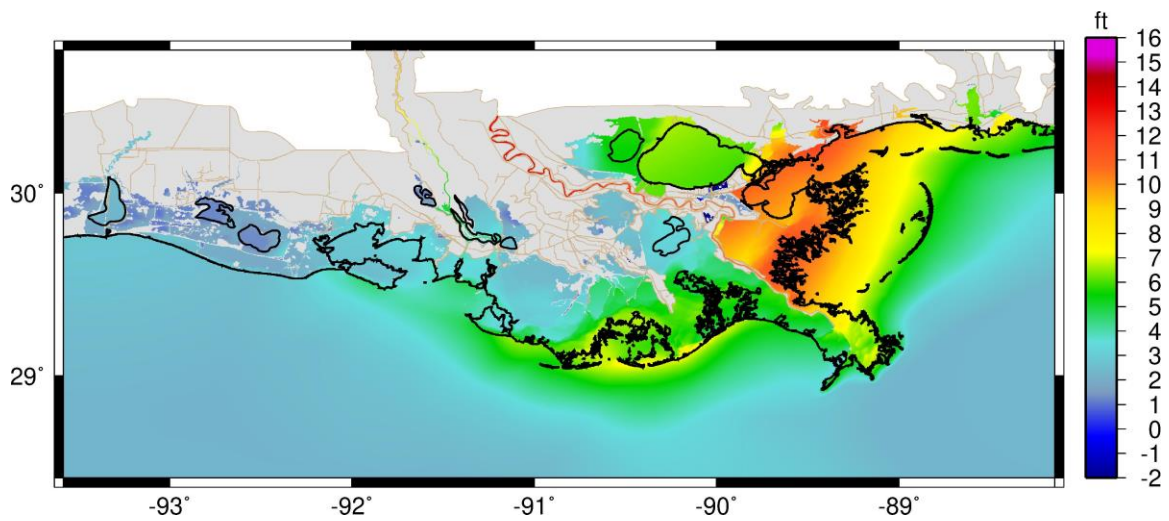


Figure 12. Maximum water surface elevation from the simulation of Hurricane Gustav using parameter set 5 (ft, NAVD88 2009.55).

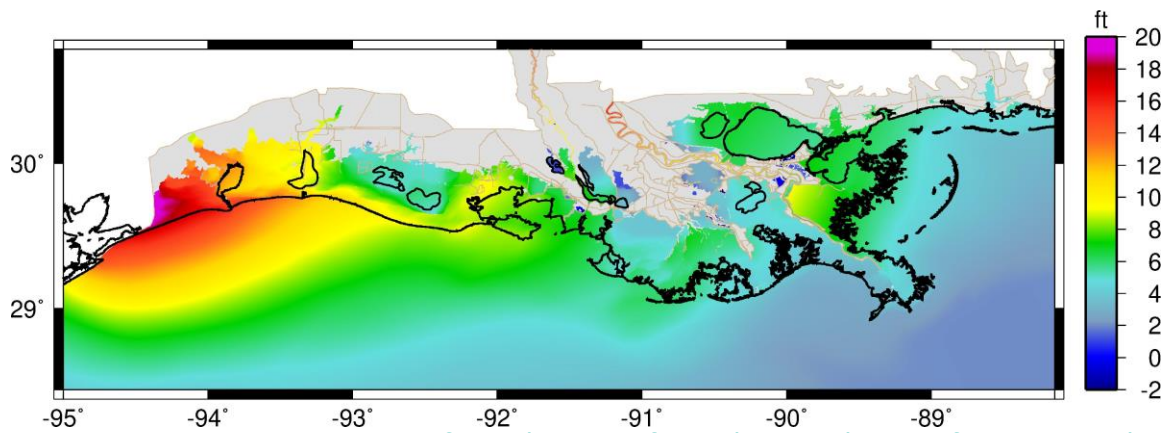


Figure 13. Maximum water surface elevation from the simulation of Hurricane Ike using parameter set 5 (ft, NAVD88 2009.55).

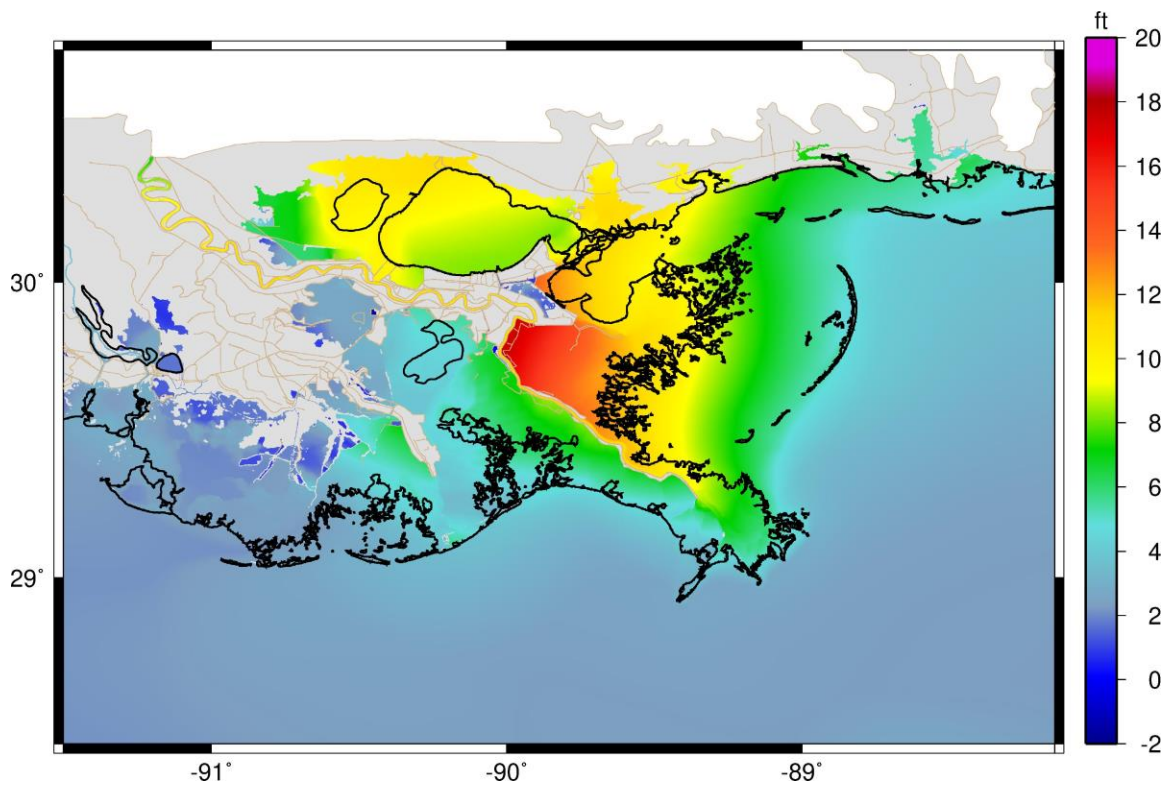


Figure 14. Maximum water surface elevation from the simulation of Hurricane Isaac using parameter set 5 (ft, NAVD88 2009.55).

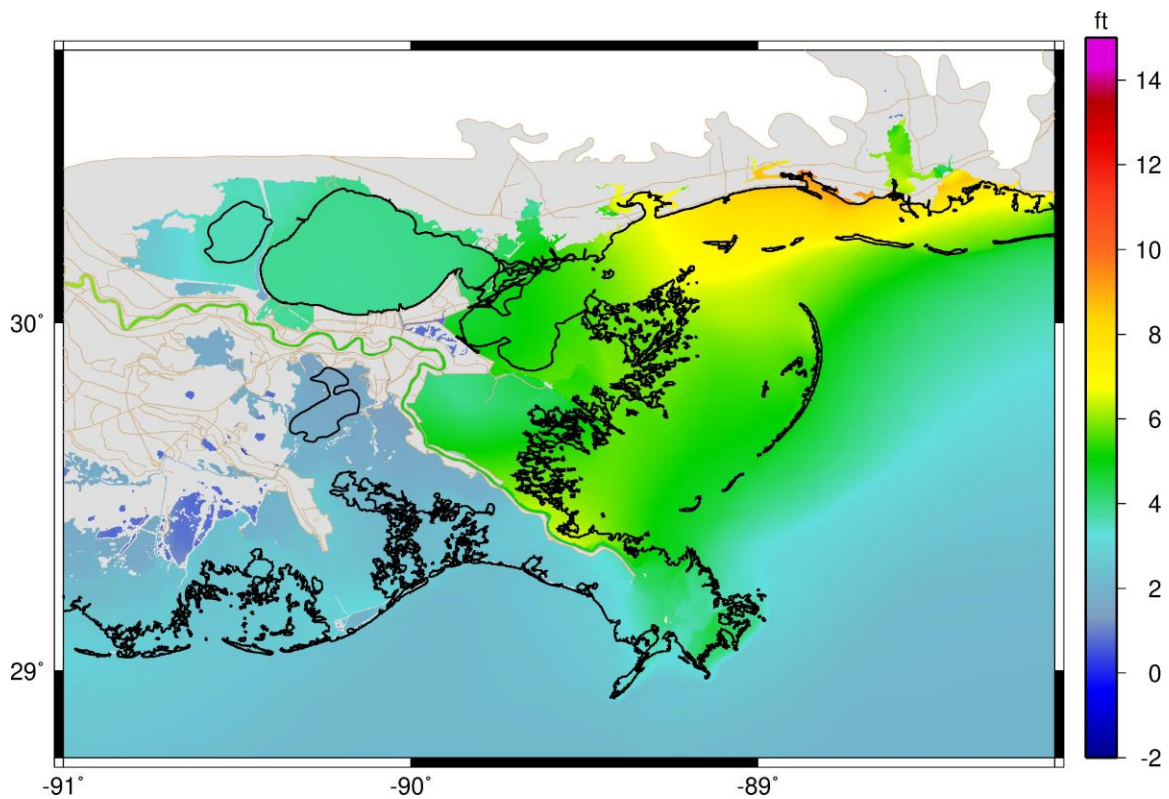


Figure 15. Maximum water surface elevation from the simulation of Hurricane Nate using parameter set 5 (ft, NAVD88 2009.55).

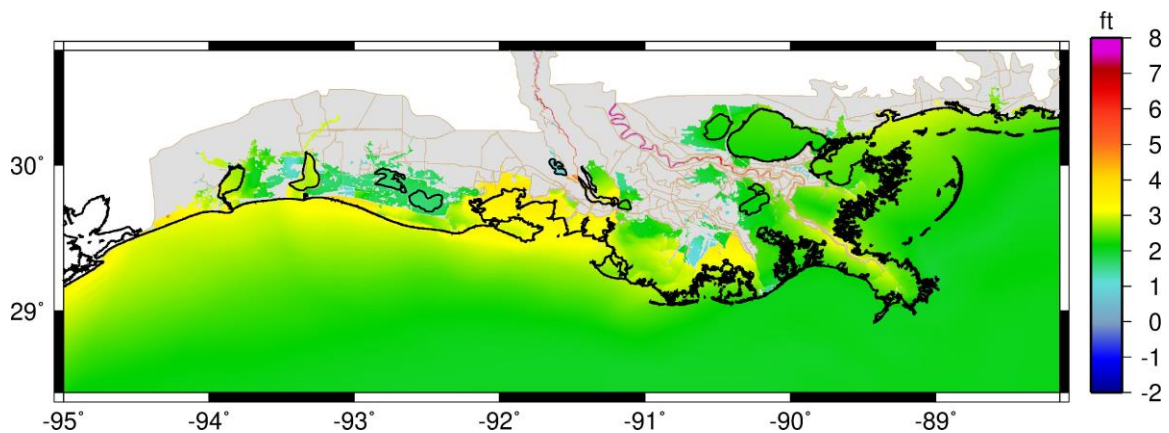


Figure 16. Maximum water surface elevation from the simulation of Hurricane Harvey using parameter set 5 (ft, NAVD88 2009.55).

HIGH-WATER MARKS COMPARISON

The comparisons of model results to high-water marks were used to understand trends in model performance based on variation of model parameters. Table 4 through Table 8 show the comparison to high-water marks for the five historical storm simulations where high-water mark data were available (Hurricanes Katrina, Rita, Gustav, Ike, Isaac). Figure 7 and Figure 17 through

Figure 20 show the comparison to high-water mark data for parameter set 5 to show the spatial distribution of available high-water marks for each storm. The high-water marks collected for Hurricane Harvey in Louisiana included the effects of extreme rainfall, and Hurricane Nate only had available high-water marks in Mississippi, these storms were included only in the timeseries analysis.

Note that comparison values for Hurricane Katrina shown in Table 3 have slight differences from those shown in Table 4 due to the change in ADCIRC code version previously mentioned.

Table 4. Modeled high-water mark comparisons for Hurricane Katrina for the selected parameter sets.

Parameter Set	Drag Formula	Air-sea drag Limit	Bottom Friction Limit	Slope	R^2	σ
4	Garratt	0.0025	0.000	1.01	0.89	1.96
5	Garratt	0.0025	0.001	0.99	0.90	1.93
9	Garratt	0.0030	0.003	0.98	0.91	1.79
*12	Garratt	0.0035	0.003	1.04	0.92	1.97
†13	Powell	n/a	0.000	1.02	0.90	1.93
14	Powell	n/a	0.001	0.99	0.89	1.92

*FEMA 2008

†2017 Coastal Master Plan

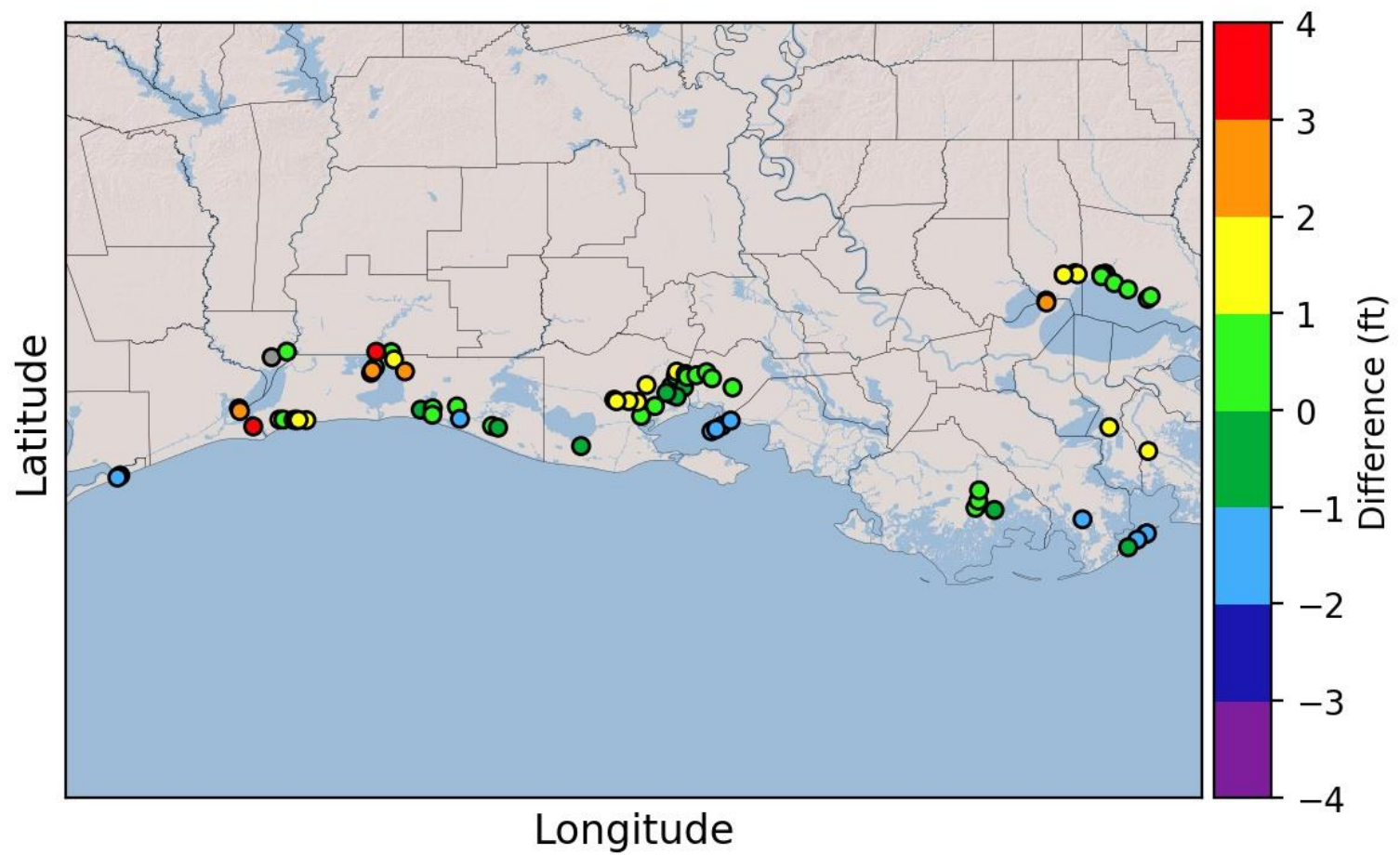


Figure 17. Hurricane Rita comparison to observed high water marks for parameter set 5.

Table 5. Modeled high-water mark comparisons for Hurricane Rita for the selected parameter sets.

Parameter Set	Drag Formula	Air-sea Drag Limit	Bottom Friction Limit	Slope	R^2	σ
4	Garratt	0.0025	0.000	1.16	0.73	1.48
5	Garratt	0.0025	0.001	1.05	0.74	1.29
9	Garratt	0.0030	0.003	0.94	0.68	1.43
*12	Garratt	0.0035	0.003	0.95	0.67	1.44
†13	Powell	n/a	0.000	1.07	0.67	1.44
14	Powell	n/a	0.001	0.97	0.65	1.37

*FEMA 2008

†2017 Coastal Master Plan

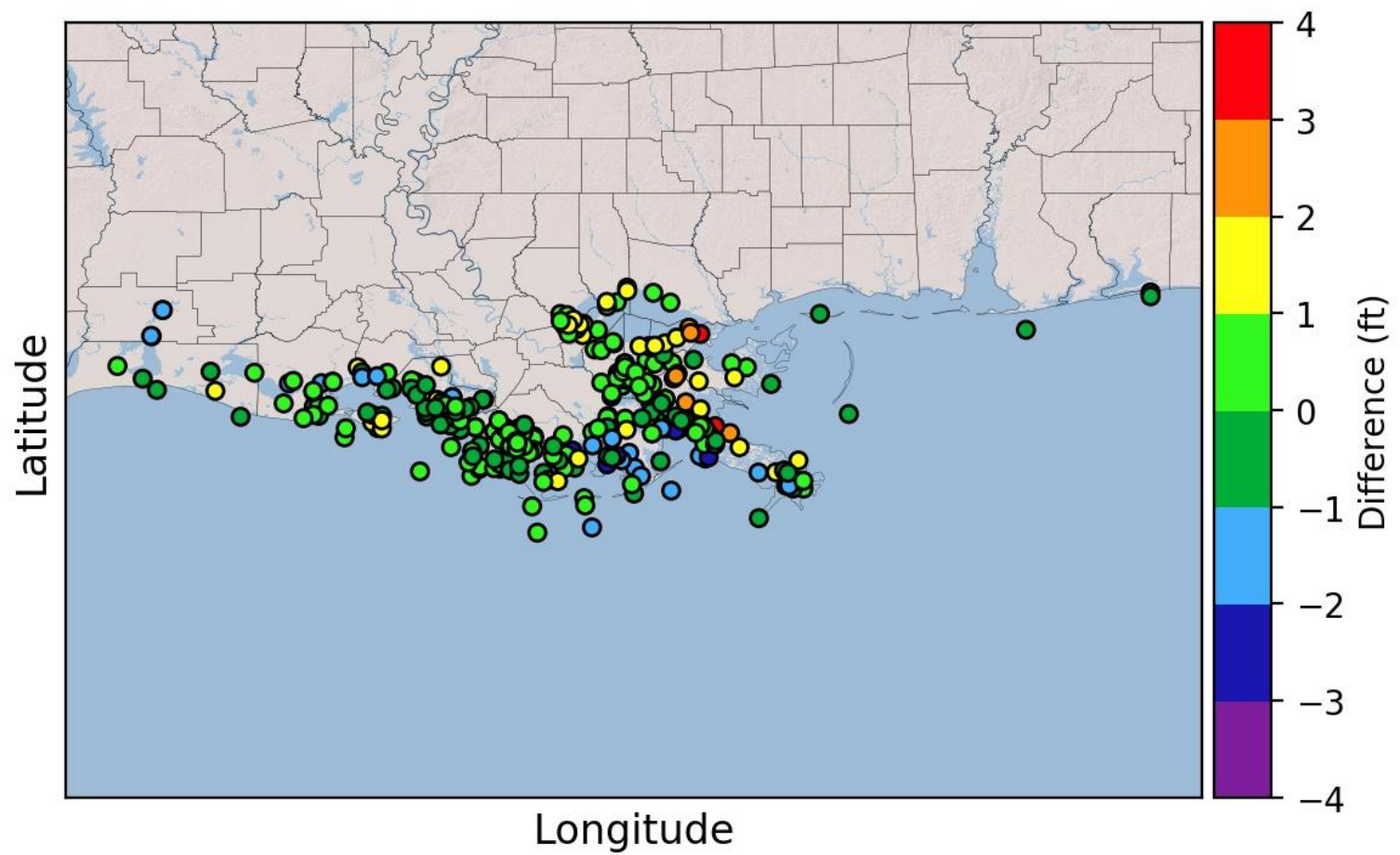


Figure 18. Hurricane Gustav comparison to observed high-water marks for parameter set 5.

Table 6. Modeled high-water mark comparisons for Hurricane Gustav for the selected parameter sets.

Parameter Set	Drag Formula	Air-sea drag Limit	Bottom Friction Limit	Slope	R^2	σ
4	Garratt	0.0025	0.000	1.05	0.78	0.96
5	Garratt	0.0025	0.001	1.01	0.78	0.96
9	Garratt	0.0030	0.003	0.94	0.78	0.92
*12	Garratt	0.0035	0.003	0.94	0.78	0.92
†13	Powell	n/a	0.000	0.99	0.75	0.94
14	Powell	n/a	0.001	0.95	0.75	0.96

*FEMA 2008

†2017 Coastal Master Plan

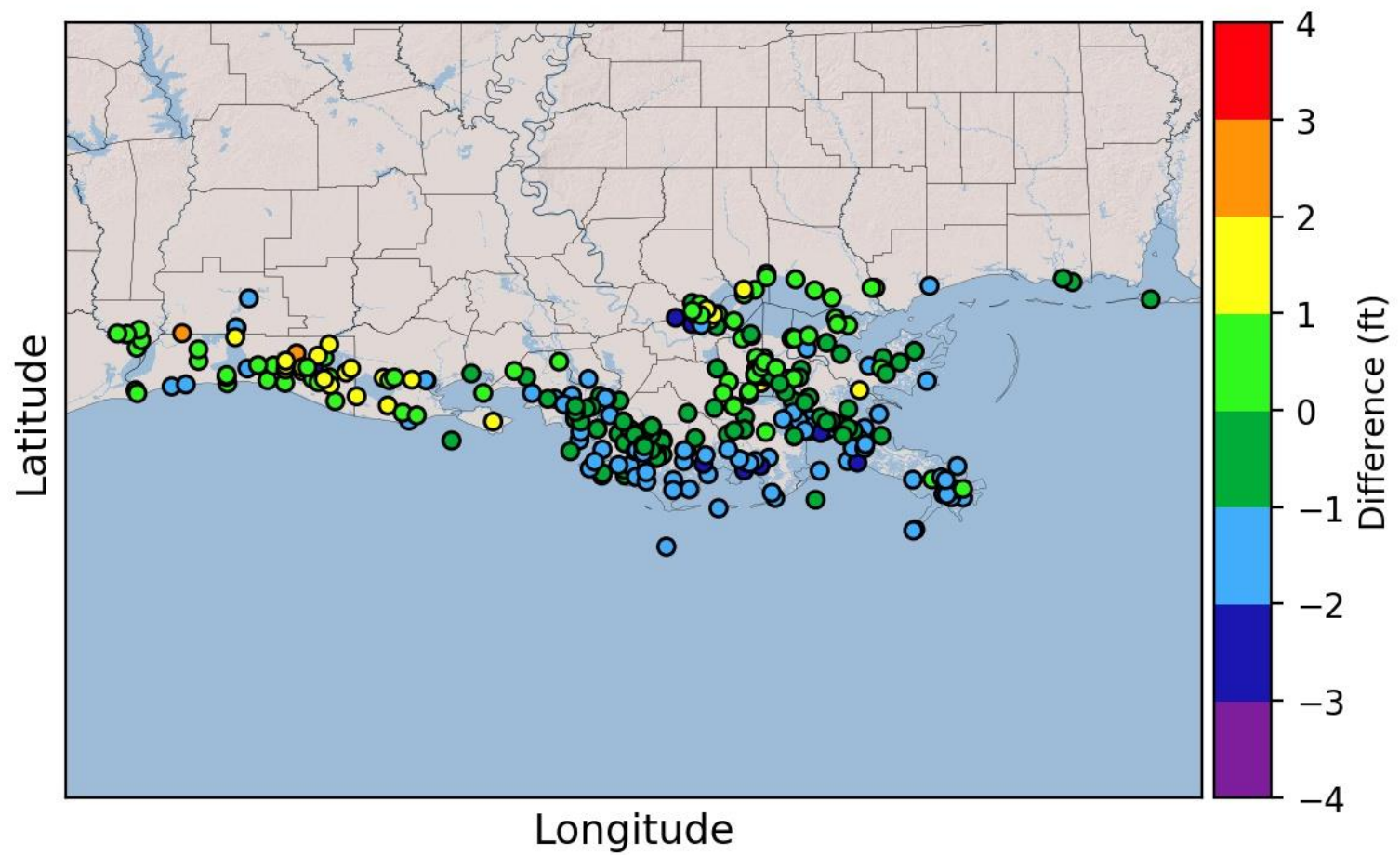


Figure 19. Hurricane Ike comparison to observed high-water marks for parameter set 5.

Table 7. Modeled high-water mark comparisons for Hurricane Ike for the selected parameter sets.

Parameter Set	Drag Formula	Air-sea drag Limit	Bottom Friction Limit	Slope	R^2	σ
4	Garratt	0.0025	0.000	1.02	0.75	1.18
5	Garratt	0.0025	0.001	0.93	0.78	0.97
9	Garratt	0.0030	0.003	0.84	0.79	0.91
*12	Garratt	0.0035	0.003	0.84	0.79	0.92
†13	Powell	n/a	0.000	0.94	0.77	0.96
14	Powell	n/a	0.001	0.87	0.76	0.93

*FEMA 2008

†2017 Coastal Master Plan

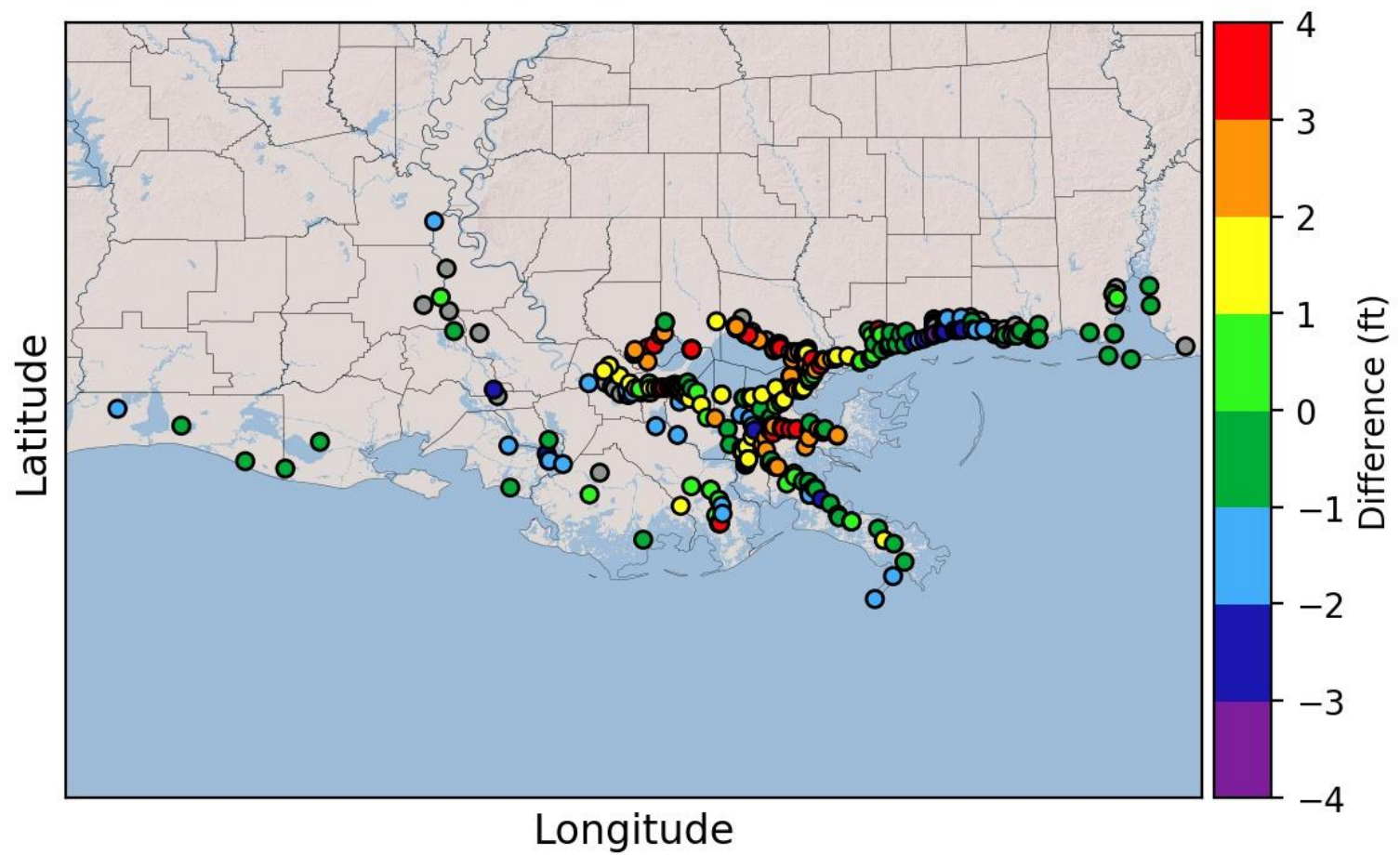


Figure 20. Hurricane Isaac comparison to observed high-water marks for parameter set 5.

Table 8. Modeled high-water mark comparisons for Hurricane Isaac for the selected parameter sets.

Parameter Set	Drag Formula	Air-sea drag Limit	Bottom Friction Limit	Slope	R^2	σ
4	Garratt	0.0025	0.000	1.14	0.69	1.87
5	Garratt	0.0025	0.001	1.12	0.69	1.84
9	Garratt	0.0030	0.003	1.08	0.72	1.74
*12	Garratt	0.0035	0.003	1.08	0.72	1.74
†13	Powell	n/a	0.000	1.04	0.68	1.63
14	Powell	n/a	0.001	1.03	0.69	1.63

*FEMA 2008

†2017 Coastal Master Plan

High-water marks across five storms were aggregated to two sets: (a) all high-water marks coastwide and (b) high-water marks only within Louisiana.

Figure 21 and Figure 22 show the aggregated high-water marks coastwide and Figure 23 and Figure 24 show the aggregated high-water marks for Louisiana only.

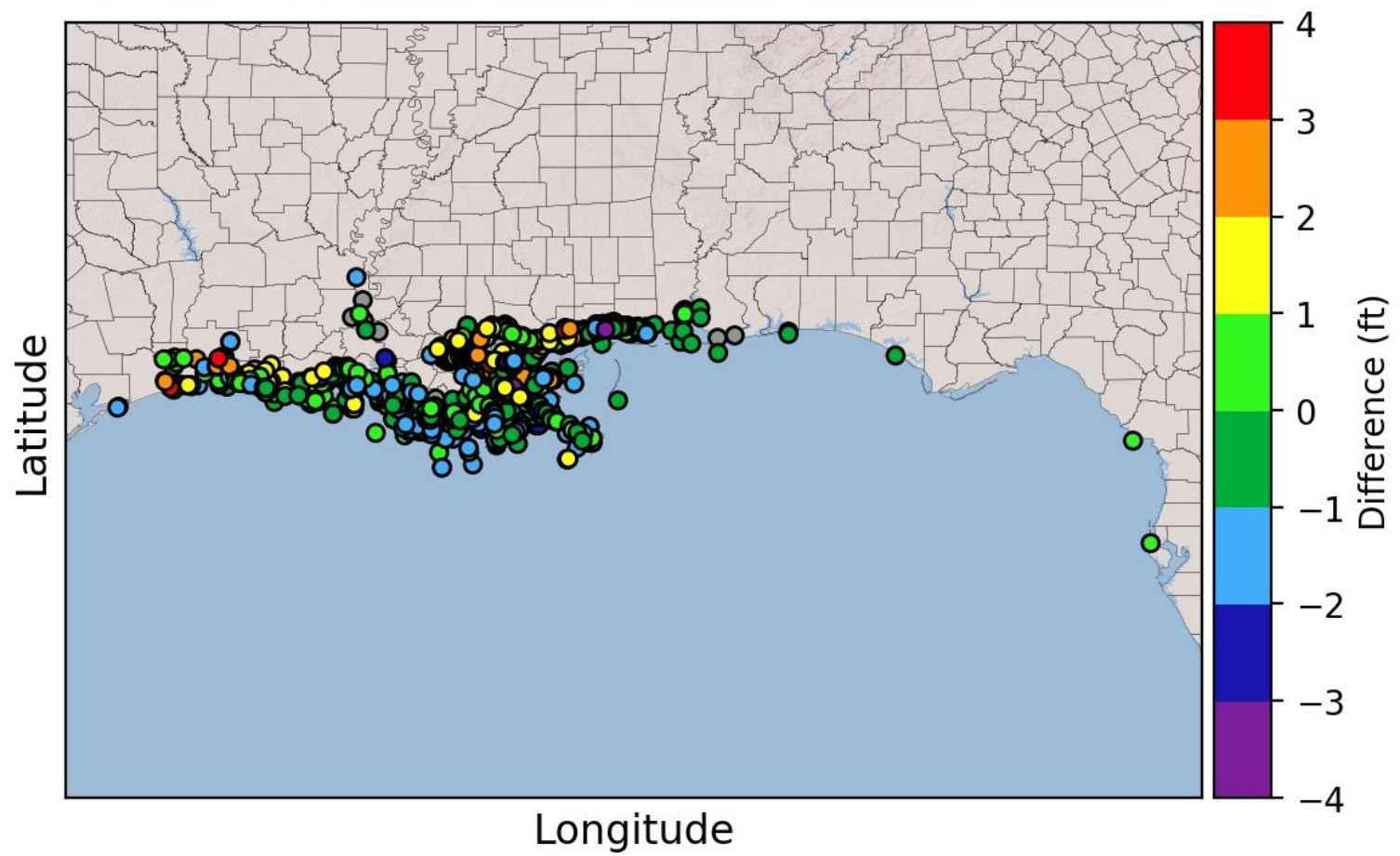


Figure 21. Aggregated coastwide high-water marks for parameter set 5.

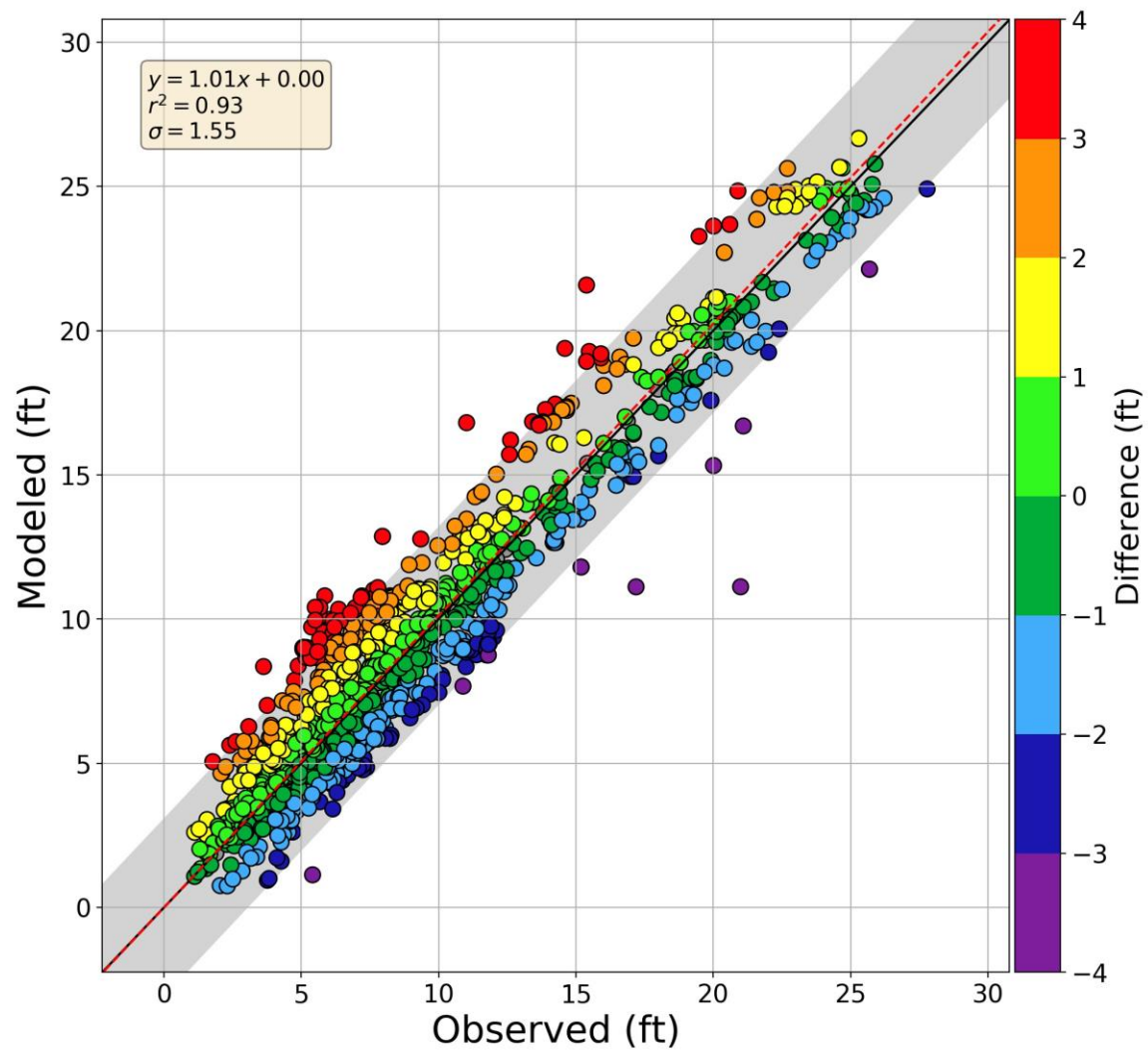


Figure 22. Aggregated coastwide high-water mark regression for parameter set 5.

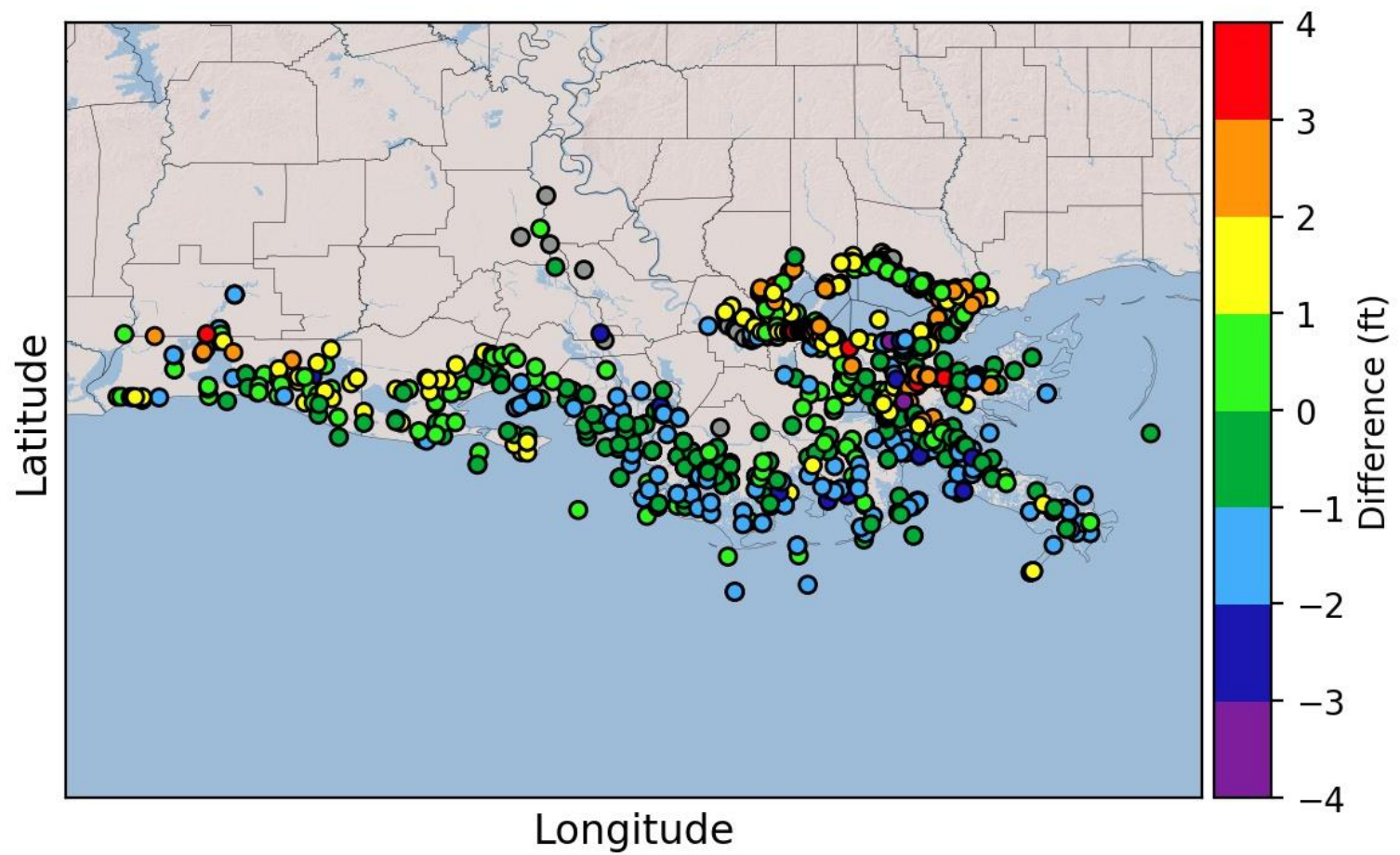


Figure 23. Louisiana-only aggregated high-water marks for parameter set 5.

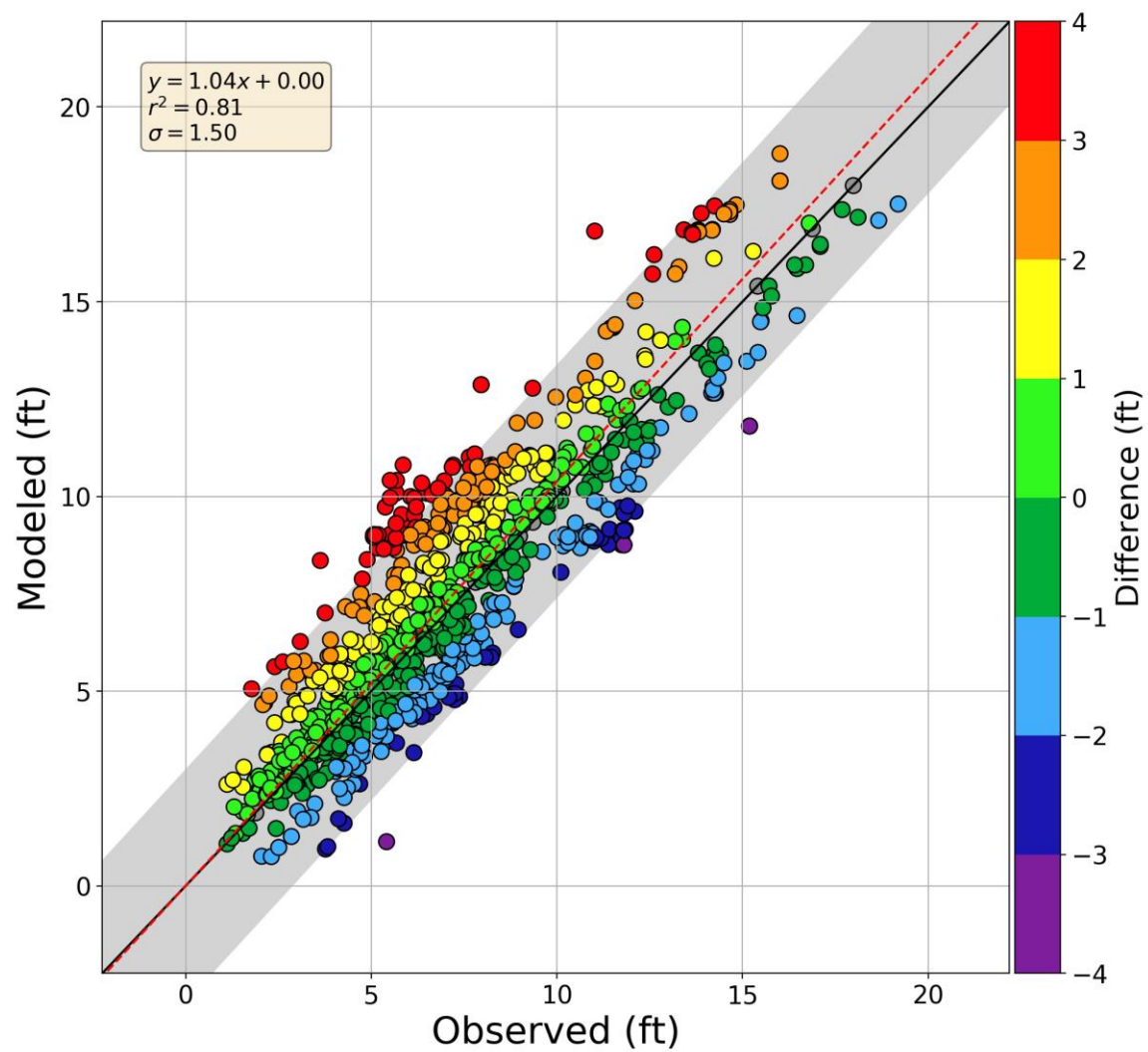


Figure 24. Louisiana-only aggregated high-water mark regression for parameter set 5.

Table 9. Aggregated high-water marks coastwide for all tested parameter sets.

Set	Drag Formula	Air-sea drag Limit	Bottom Friction Limit	Slope	R ²	σ
4	Garratt	0.0025	0.000	1.04	0.93	1.59
5	Garratt	0.0025	0.001	1.01	0.93	1.55
9	Garratt	0.0030	0.003	0.99	0.94	1.49
*12	Garratt	0.0035	0.003	1.03	0.94	1.59
†13	Powell	n/a	0.000	1.02	0.94	1.42
14	Powell	n/a	0.001	0.99	0.94	1.42

*FEMA 2008

†2017 Coastal Master Plan

Table 10. Aggregated high-water marks in Louisiana for all tested parameter sets.

Set	Drag Formula	Air-sea drag Limit	Bottom Friction Limit	Slope	R ²	σ
4	Garratt	0.0025	0.000	1.08	0.81	1.53
5	Garratt	0.0025	0.001	1.04	0.81	1.50
9	Garratt	0.0030	0.003	0.97	0.81	1.48
*12	Garratt	0.0035	0.003	0.98	0.81	1.47
†13	Powell	n/a	0.000	1.03	0.85	1.31
14	Powell	n/a	0.001	0.99	0.84	1.33

*FEMA 2008

†2017 Coastal Master Plan

TIMESERIES COMPARISON

In addition to comparing high-water mark locations, water level data generated by the model were also compared to observational data, including peak storm values and trends pre- and post-storm.

Evaluation of the water surface elevation time series for the rising and falling limbs of the hydrograph is critical to assess the model representation of important physical processes like those at play during the forerunner that occurred prior to Hurricane Ike. This is important so that the model can be shown to be replicating the physics rather than being purely tuned to reproducing peak elevations, where it would be possible to generate well matched high water marks but not replicate the physical processes well.

Figure 25 and Figure 26 show water levels during Hurricane Katrina on the north side of the IHNC

Lock, demonstrating surge patterns in the corridor that once connected Lake Borgne and Lake Pontchartrain via the IHNC and Gulf Intracoastal Waterway (GIWW) during storms prior to HSDRRS system upgrades. Garratt-based formulations are shown as solid lines and Powell formulations are shown as dashed lines. The Garratt formulations with highest combinations of drag and bottom friction emphasized the double-peaked hydrograph which does not appear in the data, while lower drag formulations approached a single peak, similar to that shown in the water level observation data. All formulations tend to show similar drainage rates after the storm has passed.

Figure 27 and Figure 28 show simulations of Hurricane Gustav and the modeled water levels at Southwest Pass. In this case, all Garratt-based formulations overpredicted the observed water levels while the Powell formulations underpredicted. Also, note that the formulations do not diverge until the storm is near the coast, meaning that both tides and pre-storm winds are not overly sensitive to the selection of air-sea drag and bottom friction formulation.

The 2011 storm surge study in Texas (USACE, 2011) was in progress when Hurricane Ike made landfall and the modeling team undertook a validation of the storm finding that the model was unable to replicate a forerunner surge, caused by strong shore parallel winds which propagated a geostrophic wave along the Louisiana and Texas coasts, elevating water levels before the storm made landfall. The USACE study demonstrated that ADCIRC parameterizations like parameter set 12 in this study did not capture the forerunner, while parameterizations like parameter sets 4 and 5 were better able to replicate the forerunner. Observations near Sabine Pass, shown in Figure 29 and Figure 30, capture the initial rise in water level, or forerunner, before the storm's landfall. While none of the model parameterizations perfectly captured the forerunner, the models with high bottom friction coefficients did not generate any part of the forerunner signal. The model results for parameter set 4 provided a simulation of the forerunner that was most consistent with observations, however that parametrization overpredicted the peak surge considerably. Model results for parameter sets 5 and 13 represented both the forerunner and the peak surge well, with parameter set 13 most accurately capturing the forerunner and peak surge.

Figure 31 through Figure 34 show observed and modeled time series for Hurricanes Nate and Harvey. Both storms generated relatively low storm surge levels within Louisiana. Model outputs for the six parameterizations for Hurricane Harvey showed relatively little separation between the modeled time series because the winds are not as strong as other storms. However, due to much stronger winds, modeled time series showed variation across the parameterizations for Hurricane Nate, particularly during the peak of the storm, though the bottom friction.

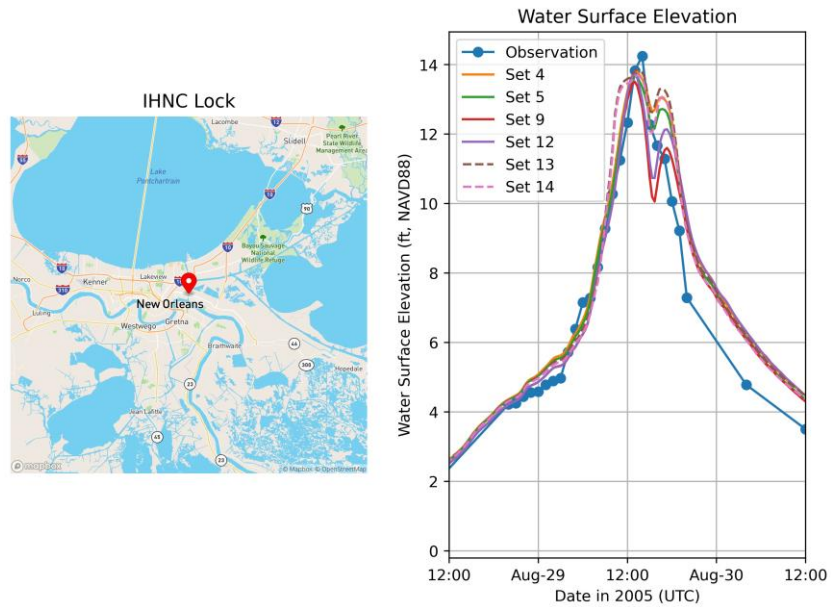


Figure 25. Modeled and observed water levels during Hurricane Katrina near the IHNC Lock. Parameter set numbers in the figure refer to Table 3.

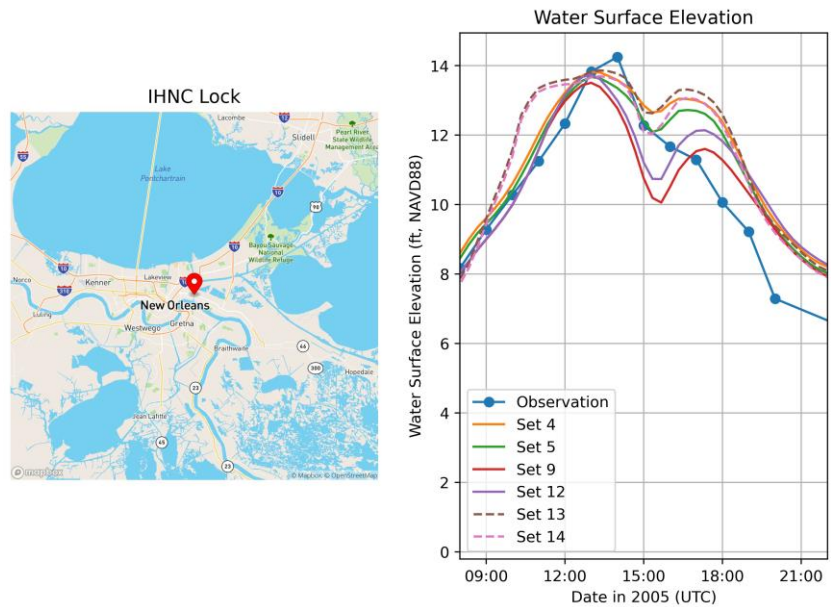


Figure 26. Modeled and observed water levels during Hurricane Katrina near the IHNC Lock near the time of peak surge. Parameter set numbers in the figure refer to Table 3.

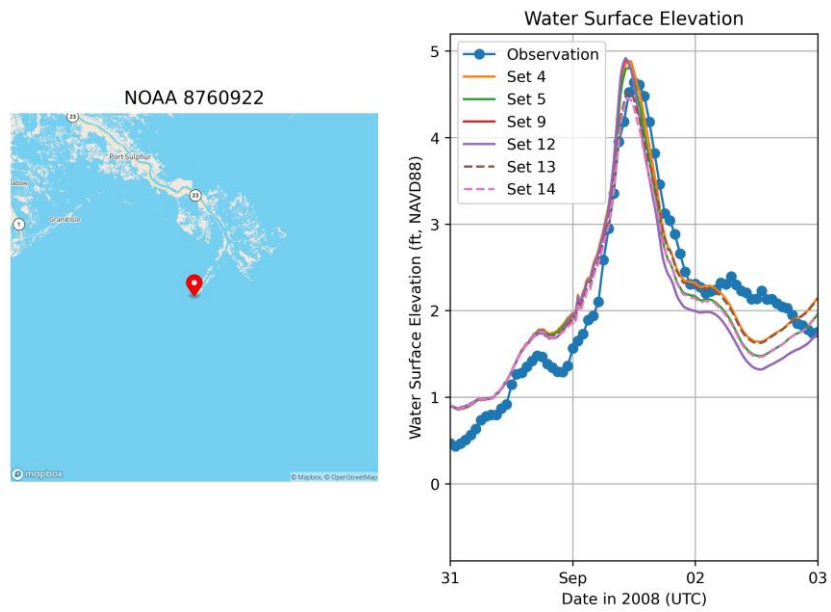


Figure 27. Hurricane Gustav modeled and observed water levels at Southwest Pass.

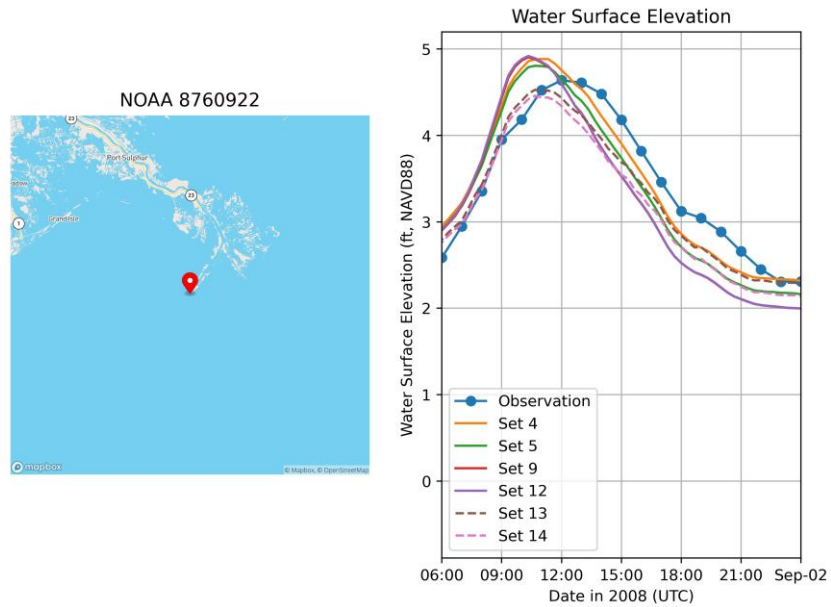


Figure 28. Hurricane Gustav modeled and observed water levels at Southwest Pass near the time of peak surge. Parameter set numbers in the figure refer to Table 3.

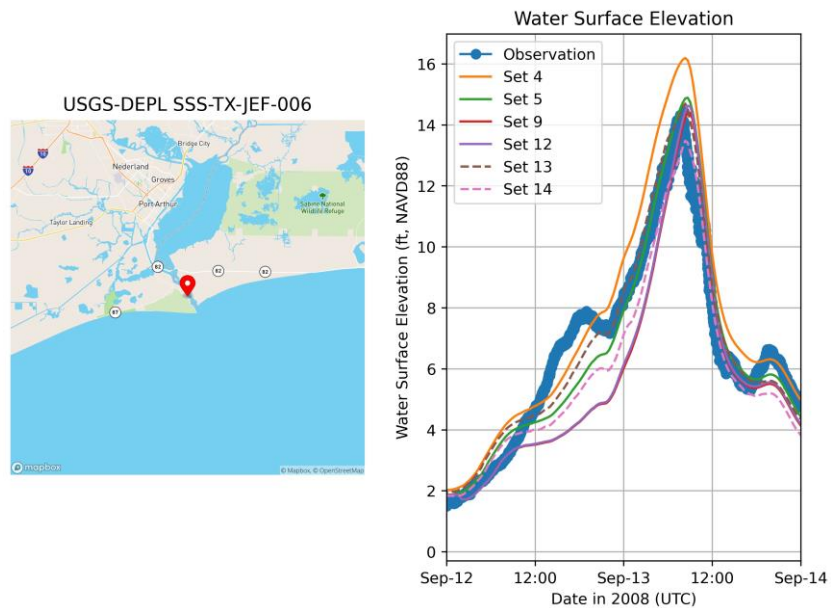


Figure 29. Hurricane Ike modeled and observed water levels at Sabine Pass. Parameter set numbers in the figure refer to Table 3.

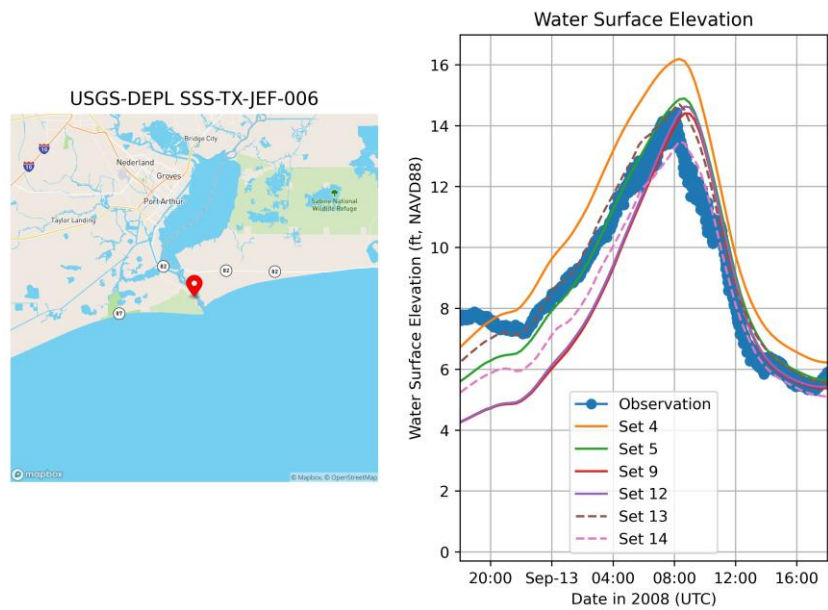


Figure 30. Hurricane Ike modeled and observed water levels at Sabine Pass near the time of peak surge. Parameter set numbers in the figure refer to Table 3.

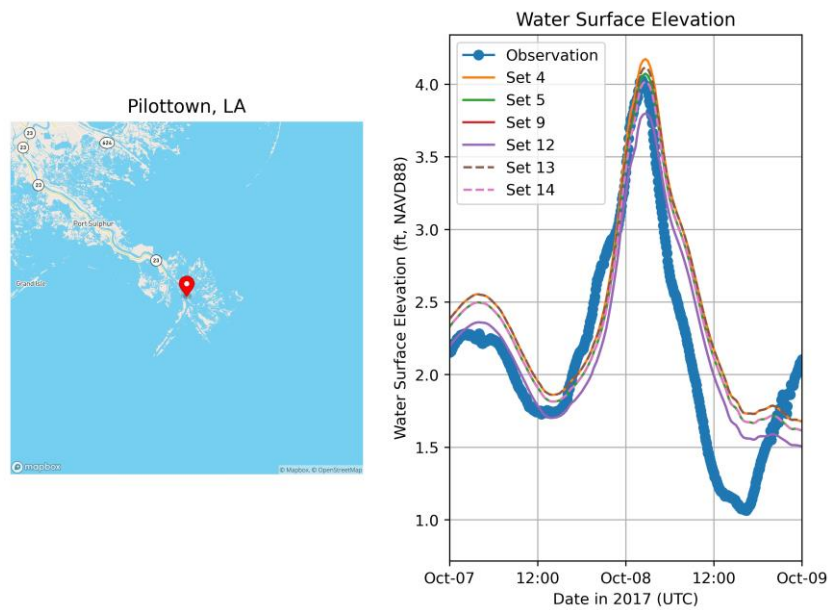


Figure 31. Hurricane Nate modeled and observed water levels at Pilottown. Parameter set numbers in the figure refer to Table 3.

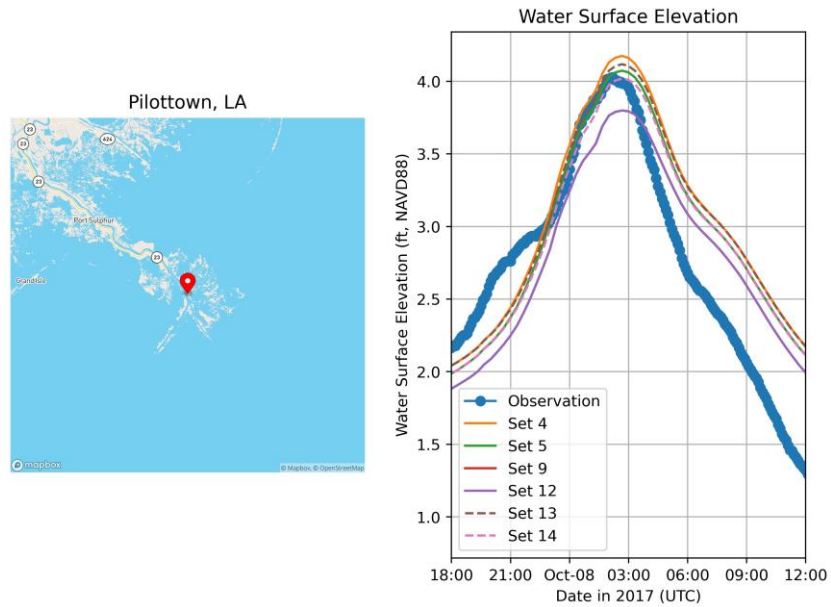


Figure 32. Hurricane Nate modeled and observed water levels at Pilottown near the time of peak surge. Parameter set numbers in the figure refer to Table 3.

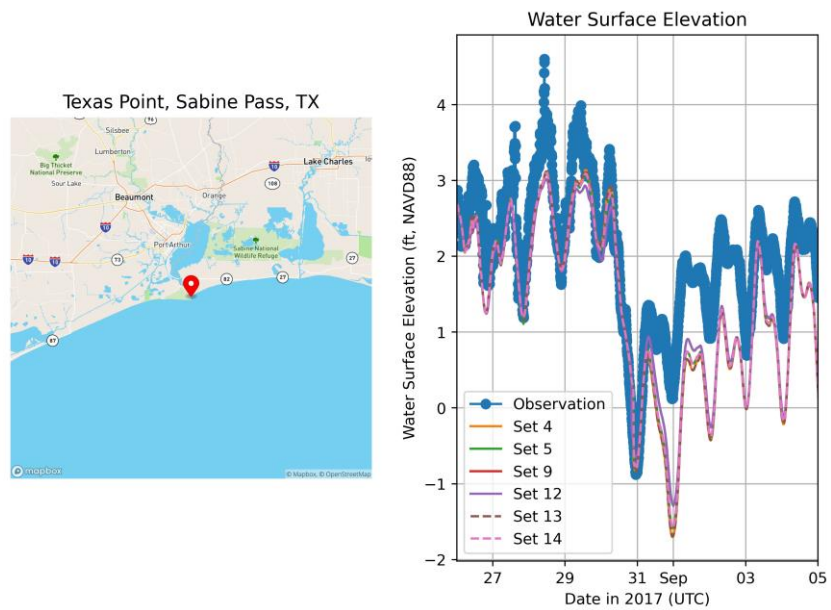


Figure 33. Hurricane Harvey modeled and observed water levels at Calcasieu Pass. Parameter set numbers in the figure refer to Table 3.

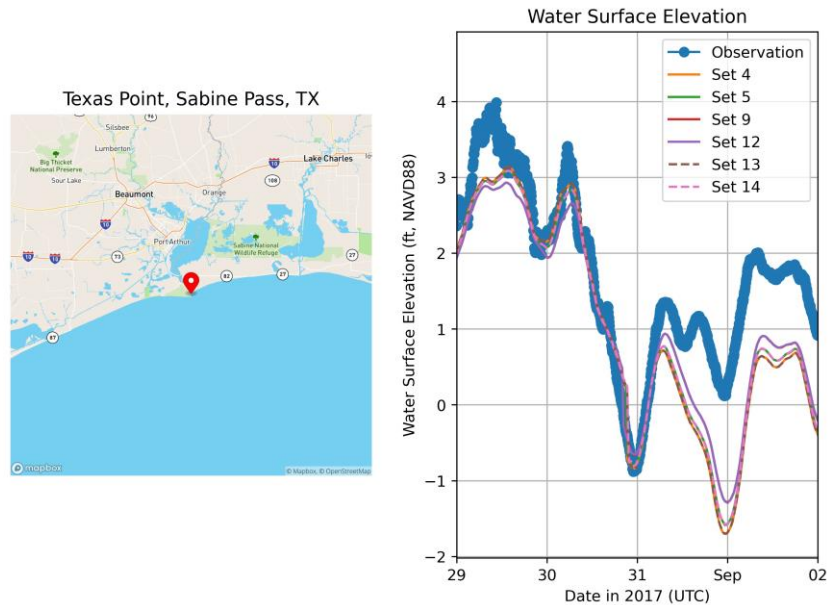


Figure 34. Hurricane Harvey modeled and observed water levels at Calcasieu Pass near the time of landfall. Parameter set numbers in the figure refer to Table 3.

RECOMMENDATION

Two formulations demonstrate broad applicability throughout the range of historic storm events. Parameter sets 5 and 13 show the best performance in terms of both high-water mark and time series comparisons. Parameter set 13 was used in the 2017 Coastal Master Plan and does show the best overall agreement between modeled and observed data. However, this formulation is specific to hurricanes with a well-defined vortex, as it approximates wave direction relative to the center of the storm. Accordingly, it does not provide for the simulation of other types of storm events which are of interest throughout various studies conducted in Louisiana (i.e., non-tropical storms). Because the ADCIRC model developed for the master plan has potential uses beyond synthetic hurricane events, it is recommended that parameter set 5 be used so that the model configuration can be broadly applicable to many types of events. Future studies might examine more advanced representations of air-sea drag coefficients, such as those proposed by Holthuijsen, which may be able to consider wave-driven processes not only during hurricanes, but other events as well. Additionally, the interaction of three-dimensional effects on roughness values during energetic events remains an area of active research (Reid, 1957; Tritinger, 2019), and these advancements should likewise be monitored for inclusion in future work.

3.0 INITIAL AND BOUNDARY CONDITIONS

As part of the ADCIRC model setup, the primary initial and background conditions considered are inflows from the Mississippi and Atchafalaya Rivers and initial water levels for the Gulf of Mexico. The river inflows establish stages along their length and account for compound fluvial and coastal effects at their outlets which can be important for the evaluation of annual exceedance probabilities (AEPs) in adjacent areas. For historical events, like those described in Section 2, the initial conditions are storm specific for both the Gulf and rivers. Initial conditions are defined based on historical observations representative of the period.

3.1 RIVER FLOW RATES

Like the 2017 Coastal Master Plan, the 2023 Coastal Master Plan ADCIRC model simulates flows within the Mississippi and Atchafalaya Rivers to account for their impact on total water levels. The 2017 Coastal Master Plan relied upon statistical analysis from previous FEMA and USACE analyses (Federal Emergency Management Agency Region Six, and the U.S. Army Corps of Engineers, 2008; Roberts & Cobell, 2017). Recent analysis by USACE-MVN suggests that the use of a flow rate of 400,000 cubic feet per second (cfs) for the Mississippi River is appropriate for a study like the 2023 Coastal Master Plan (Agnew 2020, pre-publication). The USACE-MVN analysis evaluated water surface elevation AEPs along the Mississippi River that were created based on the simulation of a full suite of synthetic hurricanes with multiple, varying Mississippi River flow rates and the Joint Probability Method with Optimum Sampling (JPM-OS) statistical method. A single flow rate of 400,000 cfs was identified as suitable for planning studies because the simulation of the same full suite of synthetic hurricanes, combined with a single flow rate of 400,000 cfs, resulted in 1% AEPs along the Mississippi River similar to the 1% AEPs that were estimated based on the simulation of a full suite of synthetic hurricanes with multiple, varying Mississippi River flow rates.

For the 2023 Louisiana Coastal Master Plan, the Mississippi River flow rate is set at 400,000 cfs and the Atchafalaya River uses a corresponding flow rate of 171,500 cfs. The same flow rates are recommended for the 2023 Coastal Master Plan production simulations.

3.2 OFFSHORE WATER LEVELS

The initial water levels in the ADCIRC model serve two purposes. First, they define the offset between the model vertical datum (NAVD88 2009.55) and mean sea level. Second, they account for the offset between mean sea level and the mean water level of the Gulf of Mexico during hurricane season, which varies due to prevailing currents and thermal expansion.

The initial water levels used in 2012 and 2017 Coastal Master Plans are based on the FEMA analysis in Louisiana, which used data from the post-Katrina IPET analysis (Federal Emergency Management Agency Region Six, and the U.S. Army Corps of Engineers, 2008). The IPET analysis used a series of benchmark stations near New Orleans to define a local mean sea level offset of 0.44 ft in NAVD88 2004.65. FEMA then used this value plus an additional 0.66ft seasonal adjustment and an additional 0.1 ft for uncertainty. The total water level offset used for both the 2012 Coastal Master Plan analysis and the FEMA analysis was 1.2 ft NAVD88 2004.65.

For the 2017 Coastal Master Plan, the initial water level value of 1.2 ft was updated from NAVD88 2004.65 to 2009.55 using the adjustment proposed by the USACE-MVN (USACE, 2014). An adjustment of -0.17 ft was applied for a total sea level offset of 1.03 ft NAVD88 2009.65. This value was used in the 2017 Coastal Master Plan.

To update the initial water level from the value used in the 2017 Coastal Master Plan, multiple approaches were considered. First, the initial water level estimate from the 2017 Coastal Master Plan was adjusted to account for sea level rise from 2008 to 2020. Note that 2020 is the base year for the 2023 Coastal Master Plan. Second, a regional re-evaluation was completed to leverage additional data that are available through a longer period of record for the gages used in the initial IPET analysis and the additional gages that have come online through the CRMS networks since the original analysis.

The first approach assumed a linear trend of 0.09 in/yr (Figure 35), and therefore to adjust between 2008 to 2020, 0.09 ft was added to the IPET value for a total adjustment of 1.12 ft NAVD88 2009.65. The Pensacola, Florida station was used to determine the sea level rise trend because subsidence at that station is understood to be minimal relative to subsidence rates within Louisiana, while the sea level trends observed in Pensacola are similar to those in other areas of the Gulf. Stations within Louisiana observe the combined effects of eustatic sea level rise and subsidence, making it difficult to rely on those gage data in this instance.

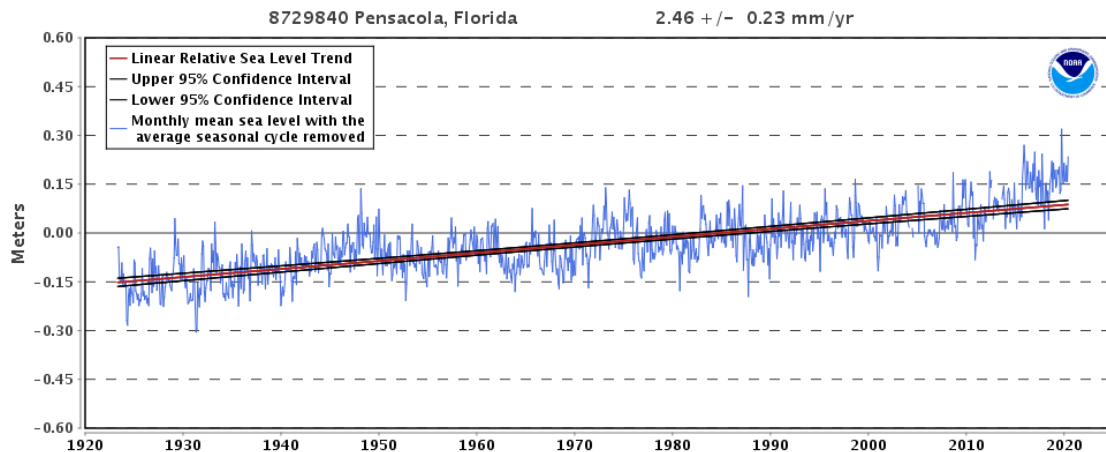


Figure 35. Relative sea level trend at NOAA 8729840 in Pensacola, FL.

The second approach used hourly water level data to generate mean sea level values for each station in the CRMS network for a tidal datum epoch between January 1, 2015 and January 1, 2020, provided that the station has at least four years of available data. Figure 36 shows all stations which have available data for the tidal epoch period. However, stations set back from the coastline likely contain the influence of rainfall, river inflows, impoundments, and other processes that are not representative of Gulf of Mexico water levels. The stations were filtered for coastal stations only as shown in Figure 37. The average of the computed mean sea level values is 0.53 ft NAVD88 2009.65. Using the seasonal offset of 0.66 ft described above, the total water level is 1.19 ft NAVD88 2009.65 based on this re-evaluation approach.

The two approaches provide similar values (within an inch of one another). For the purposes of the 2023 Coastal Master Plan analysis, the value computed from the CRMS network (1.19 ft NAVD88 2009.65) has been selected such that local data are used to inform the assessment.

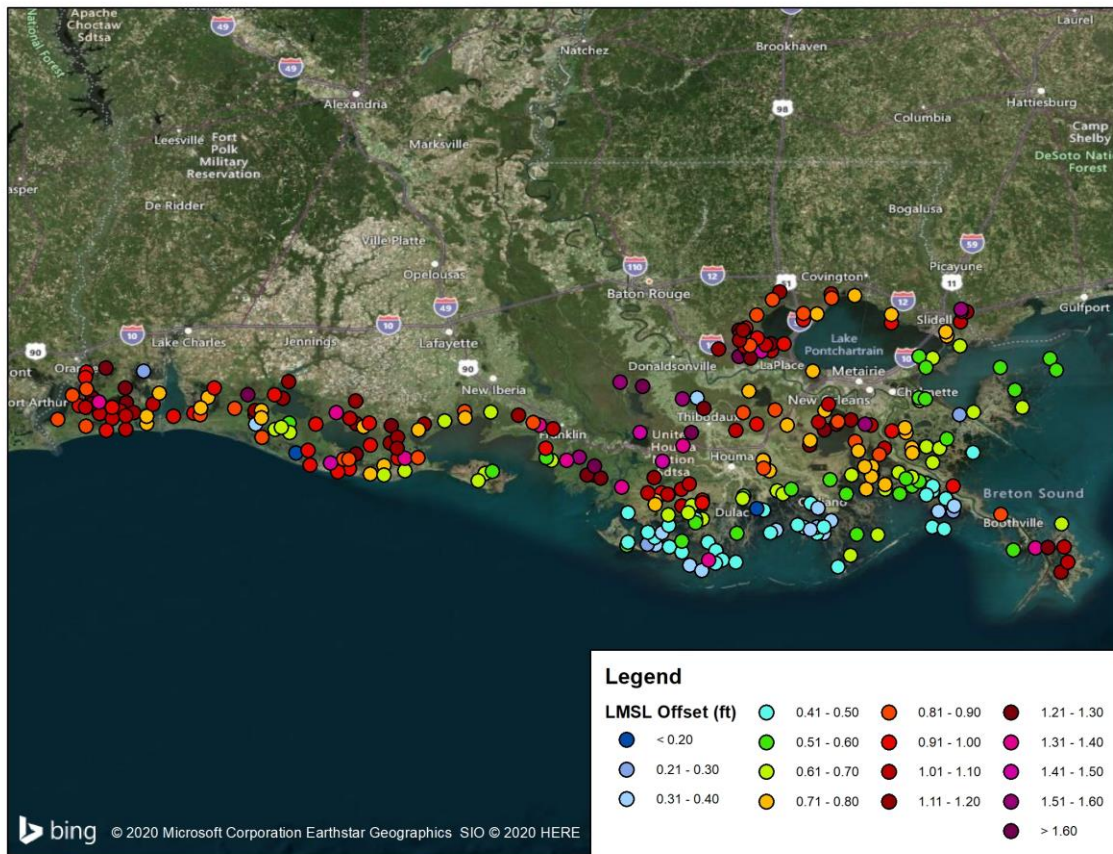


Figure 36. Computed mean sea level offset from NAVD88 2009.55 values at all available stations in the CRMS network.

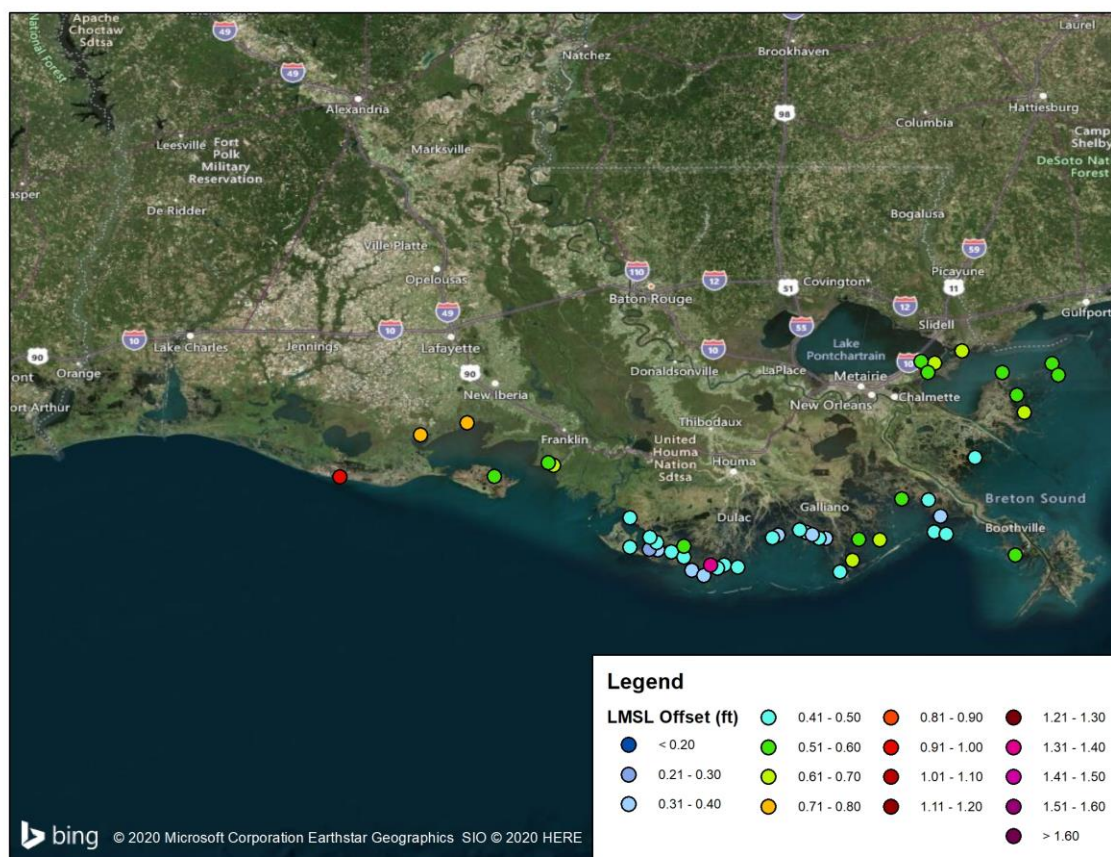


Figure 37. Computed mean sea level offset from NAVD88 2009.55 at coastal stations in the CRMS network.

4.0 REFERENCES

- Dietrich, J. C., Tanaka, S., Westerink, J. J., Dawson, C. N., Luettich, R. A., Zijlema, M., Holthuijsen, L. H., Smith, J. M., Westerink, L. G., & Westerink, H. J. (2011a). Performance of the unstructured-mesh, SWAN+ADCIRC model in computing hurricane waves and surge. *Journal of Scientific Computing*, 52, 468–497.
- Dietrich, J. C., Westerink, J. J., Kennedy, A. B., Smith, J. M., Jensen, R. E., Zijlema, M., Holthuijsen, L. H., Dawson, C., Luettich, R. A., Powell, M. D., Cardone, V. J., Cox, A. T., Stone, G. W., Pourtaheri, H., Hope, M. E., Tanaka, S., Westerink, L. G., Westerink, H. J., & Cobell, Z. (2011b). Hurricane Gustav (2008) waves and storm surge: hindcast, synoptic analysis, and validation in southern Louisiana. *Monthly Weather Review*, 139(8), 2488–2522.
- Federal Emergency Management Agency Region Six, and the U.S. Army Corps of Engineers. (2008). *Flood Insurance Study: Southeastern Parishes, Louisiana, Intermediate submission 2: Offshore water levels and waves* (p. 192).
- Garratt, J. R. (1977). Review of drag coefficients over oceans and continents. *Monthly Weather Review*, 105, 915–929.
- Holthuijsen, L. H., Powell, M. D., & Pietrzak, J. D. (2012). Wind and waves in extreme hurricanes. *Journal of Geophysical Research*, 117(C09003), 15.
- Hope, M. E., Westerink, J. J., Kennedy, A. B., Kerr, P. C., Dietrich, J. C., Dawson, C., Bender, C. J., Smith, J. M., Jensen, R. E., Zijlema, M., Holthuijsen, L. H., Luettich Jr., R. A., Powell, M. D., Cardone, V. J., Cox, A. T., Pourtaheri, H., Roberts, H. J., Atkinson, J. H., Tanaka, S., Westerink, H. J., & Westerink, L. G. (2013). Hindcast and validation of Hurricane Ike (2008) waves, forerunner, and storm surge. *Journal of Geophysical Research: Oceans*, 118(9), 4424–4460.
- Luettich, R. A., & Westerink, J. J. (2004). *Formulation and numerical implementation of the 2D/3D ADCIRC Finite Element Model* (p. 74). Chapel Hill, NC: University of North Carolina at Chapel Hill, University of Notre Dame.
- Powell, M. D. (2007). *Drag coefficient distribution and wind speed dependence in tropical cyclones* (Final Report) (p. 26). Miami, FL: National Oceanographic and Atmospheric Administration Joint Hurricane Testbed (JHT) Program.

- Reid, R. O. (1957). *Modification of the Quadratic Bottom-Stress Law for Turbulent Channel Flow in the Presence of Surface Wind Stress* (Technical Memorandum No. 93) (p. 47). College Station, TX: A&M College of Texas.
- Roberts, H., & Cobell, Z. (2017). *2017 Coastal Master Plan: Attachment C3-25.1: Storm surge* (Version Final) (pp. 1–110). Baton Rouge, LA: Coastal Protection and Restoration Authority.
- Tritinger, A. (2019). *The Influence of Vertical Current Structure on Wind-Driven Surges in the Nearshore Region*. University of Florida, Gainesville, Florida.
- USACE. (2011). *Flood Insurance Study: Coastal Counties, Texas Intermediate Submission 2* (p. 150). Vicksburg, MS.
- USACE. (2014). *Elevations for Design of Hurricane Protection Levees and Structures, Appendices* (p. 524). New Orleans, LA: New Orleans District.
- Wu, J. (1982). Wind-stress coefficients over sea surface from breeze to hurricane. *Journal of Geophysical Research: Oceans*, 87(C12), 9704–9706.
- Yang, Z., Myers, E., & White, S. (2010). *VDatum For Eastern Louisiana And Mississippi Coastal Waters: Tidal Datums, Marine Grids, And Sea Surface Topography* (No. NOAA Technical Memorandum NOS CS 19). National Oceanic and Atmospheric Administration.